Astrochemistry

Millar, T. J. (2015). Astrochemistry. *Plasma Sources Science and Technology*, *24*(4), [043001]. https://doi.org/10.1088/0963-0252/24/4/043001

Published in:
Plasma Sources Science and Technology

Document Version:
Publisher's PDF, also known as Version of record

Queen's University Belfast - Research Portal:
Link to publication record in Queen's University Belfast Research Portal

Astrochemistry

2015 Plasma Sources Sci. Technol. 24 043001

(http://iopscience.iop.org/0963-0252/24/4/043001)

OPEN ACCESS
IOP Publishing
Plasma Sources Science and Technology
Plasma Sources Sci. Technol. **24** (2015) 043001 (31pp)
doi:10.1088/0963-0252/24/4/043001

Topical Review

Astrochemistry

T J Millar

Astrophysics Research Centre, School of Mathematics and Physics, Queen's University Belfast, University Road, Belfast BT7 1NN, UK

E-mail: tom.millar@qub.ac.uk

Received 2 April 2015
Accepted for publication 18 May 2015
Published 14 July 2015

Abstract

In the last 40 years a wide range of molecules, including neutrals, cations and anions, containing up to 13 atoms—in addition to detections of C_{60} and C_{70}—have been found in the harsh environment of the interstellar medium. The exquisite sensitivity and very high spectral and, more recently, spatial resolution, of modern telescopes has enabled the physics of star formation to be probed through rotational line emission. In this article, I review the basic properties of interstellar clouds and the processes that initiate the chemistry and generate chemical complexity, particularly in regions of star and planet formation. Our understanding of astrochemistry has evolved over the years. Before 1990, the general consensus was that molecules were formed in binary, gas-phase, or volume, reactions, most importantly ion-neutral reactions despite the very low ionization in clouds. Since then, observations have indicated unambiguously that there is also a contribution from surface processes, particularly on the icy mantles that form around refractory grain cores in cold, dense gas. The balance between these two processes depends on particular physical conditions and can vary during the life cycle of a particular volume of interstellar cloud.

The complex chemistry that occurs in space is driven mostly through interaction of the gas with cosmic ray protons, a source of ionization that enables a rich ion-neutral chemistry. In addition, I show that the interaction between the gas and the dust in cold, dense regions also leads to additional chemical complexity through reactions that take place in ices at only a few tens of degrees above absolute zero. Although densities are low compared to those in terrestrial environments, the extremely long life times of interstellar clouds and their enormous sizes, enable complex molecules to be synthesised and detected. I show that in some instances, particularly in reactions involving deuterium, the rotational populations of reactants, together with spin-selection rules, can determine the detailed abundances. Although the review is mainly focused on regions associated with star formation, I also consider chemistry in other interesting astronomical regions—in the early Universe and in the envelopes formed by mass loss during the final stages of stellar evolution.

Keywords: ion-neutral reactions, astrochemistry, interstellar medium

(Some figures may appear in colour only in the online journal)

1. Introduction

Interstellar matter comprises the material, gas and dust, between the stars in our and other galaxies.

Table 1. Solar system abundances relative to hydrogen, ionization potentials and charge state for the most common elements.

Element	Abundance	I.P. (eV)	Charge state	Element	Abundance	I.P. (eV)	Charge state
H	1	13.60	H	Na	$2.34\,10^{-8}$	5.14	Na^+
He	0.1	24.59	He	Mg	$4.17\,10^{-5}$	7.65	Mg^+
C	$2.9\,10^{-4}$	11.26	C^+	Si	$4.07\,10^{-5}$	8.15	Si^+
N	$7.9\,10^{-5}$	14.53	N	P	$3.47\,10^{-7}$	10.49	P^+
O	$5.8\,10^{-4}$	13.62	O	S	$1.82\,10^{-5}$	10.36	S^+
F	$3.39\,10^{-8}$	17.42	F	Cl	$2.14\,10^{-7}$	12.98	Cl^+

Note: In interstellar clouds, these abundances are reduced from cosmic values because all, except H, He and F, have components that are locked up in interstellar grains.

Table 2. Cloud types in the ISM with typical sizes, temperatures, number densities, column densities, visual extinction, fractional ionization and species commonly used to probe physical conditions.

Cloud type	Size (pc)[a]	T (K)	n (cm^{-3})	N_H (cm^{-2})	A_V (mag)	$f(e)$[b]	Diagnostics
Diffuse	1–3	70–100	10–100	$<10^{21}$	<1	$10^{-3}-10^{-4}$	21 cm H line H_2 UV abs C^+
Dark	1–5	8–15	10^4-10^6	10^{22}	10–20	$10^{-7}-10^{-8}$	CO, H_2CO HCN, HCO^+
Hot Core	0.01–0.1	100–300	10^7-10^9	10^{24}	5000	$<10^{-9}$	CS, CH_3OH CH_3CN, NH_3
Giant Molecular	100–500	30–70	$<10^3>$	10^{25}	—	—	CO, HCN, NH_3

[a] 1 pc = $3.086\,10^{18}$ cm.
[b] $f(e) = n(e)/n$.

1.1. Interstellar gas

In broadly defined terms the interstellar gas can be partitioned into several regions all of which are in approximate pressure equilibrium. In this section we concentrate on describing the fundamental physical properties of those regions in which molecules are found. To begin with, though, we note that the general interstellar medium (ISM) contains no photons with energies greater than the ionization potential of hydrogen (13.6 eV) since such photons, which are produced by hot stars, are absorbed entirely in the neighbourhood of each star, ionizing the surrounding gas and forming the so-called Strömgren Sphere. Table 1 presents a list of elemental abundances, ionization potentials and charge state of the elements in the diffuse ISM. Representative conditions for a variety of important cloud types are given in table 2 and the (current) list of interstellar and circumstellar molecules, some 177 firm identifications are given in table 3. In passing, we note that one of the more interesting, and recent, molecules detected is ArH^+, the first identification of a noble gas molecule in the interstellar medium. Although ^{40}Ar is the most abundant isotope on Earth, where it is formed by the beta decay of ^{40}K, Barlow *et al* (2013) detected the $J = 1$–0 and 2–1 rotational transitions of $^{36}ArH^+$ in emission towards the Crab Nebula at frequencies of 617.5 and 1234.6 GHz using the Herschel Space Observatory. The detection of this isotope is consistent with its production in the explosive nucleosynthesis that occurred in the supernova explosion that created the Crab Nebula. We see here an example of how observations of molecules can be used to probe physical conditions and, particular, the history of the gas, since much of the chemistry whose products we detect is time-dependent.

As can be seen from table 2, the regions in which molecules are found in the ISM are weakly ionised plasmas with Debye lengths that are typically macroscopic, ∼10–20 m and plasma parameter, $\Lambda \sim 10^5 - 10^6$. Despite the relative paucity of charged particles in interstellar clouds, it turns out that exothermic reactions between ions and neutrals control much, though not all, of the basic chemistry that occurs in space.

1.1.1. Diffuse interstellar clouds. Diffuse clouds are so called because they are transparent to optical photons and have visual extinctions typically less than 1 magnitude (see the definition of magnitude in section 1.2). They have number densities ∼ 100–800 cm^{-3} and line-of-sight depths of a few parsecs. (A parsec (pc) is the distance at which one astronomical unit (AU), roughly an average measure of the Earth–Sun distance, subtends an angle of one arcsec, and is equal to 3.086×10^{18} cm.) Far-ultraviolet photons also penetrate through these clouds, although extinction at FUV wavelengths is several times larger than that in the visible band, and ionize atoms with ionization potentials less 13.6 eV, most importantly in terms of abundance, C^+ and S^+. The electrons produced by this process and by photoelectric emission from the dust grains heat the gas to kinetic temperatures ∼50–100 K with cooling provided by fine-structure transitions in C^+, S^+, O and rotational de-excitations in H_2. Since C^+ is readily ionized by the photon field, the fractional ionization, $f(e) = n(e)/n$ is $\sim 10^{-4}$, a large value for an interstellar cloud.

The first molecular species identified in interstellar space, CH, CH^+ and CN, were observed through optical absorption spectroscopy around 1940. Since then a number of other, rather simple molecules, including H_2, C_2, NH, CO and H_2CO, have been detected through either absorption or, where densities are large enough to provide rotational excitation, millimetre wave emission lines. Fractional abundances of these species are typically in the range $\sim 10^{-6} - 10^{-9}$.

Table 3. Molecules detected in the gas phase in interstellar and circumstellar clouds (May 2015).

Size						
2-atom	H_2	CH	CH^+	NH	OH	OH^+
	HF	SiH(?)	SH	SH^+	HCl	HCl^+
	ArH^+	C_2	CN	CN^-	CO	CO^+
	CF^+	SiC	CP	CS	N_2(?)	NO
	SiN	PN	NS	O_2	AlO	SiO
	PO	SO	SO^+	FeO(?)	AlF	NaCl
	AlCl	SiS	KCl	NO^+(?)		
3-atom	H_3^+	CH_2	NH_2	H_2O	H_2O^+	H_2S
	H_2Cl^+	C_2H	HCN	HNC	HCO	HCO^+
	HOC^+	HCP	HCS^+	N_2H^+	HNO	HO_2
	AlOH	C_3	C_2N	C_2O	c-SiC_2	C_2P
	C_2S	NaCN	MgNC	MgCN	SiCN	SiNC
	KCN	AlNC	FeCN	OCS	N_2O	SO_2
	SiCSi					
4-atom	CH_3	NH_3	H_3O^+	PH_3	C_2H_2	H_2CN
	$HCNH^+$	H_2CO	H_2CS	H_2O_2	c-C_3H	l-C_3H
	l-C_3H^+	HCCN	HNCO	HOCN	HCNO	HMgNC
	HNCS	HSCN	HCO_2^+	C_3N	C_3N^-	C_3O
	c-SiC_3	C_3S	HCCO			
5-atom	CH_4	SiH_4	CH_2NH	CH_3O	H_2COH^+	c-C_3H_2
	H_2CCC	CH_2CN	CH_2CO	HCOOH	NH_2CN	C_4H
	C_4H^-	HC_3N	HCCNC	HNCCC	CNCHO	C_5
	SiC_4					
6-atom	C_2H_4	CH_3OH	CH_3SH	CH_3CN	CH_3NC	CH_2CNH
	HC_2CHO	NH_2CHO	H_2CCCC	HC_4H	HC_3NH^+	c-C_3H_2O
	C_5H	HC_4N	C_5N	C_5N^-	C_5S	
7-atom	CH_3NH_2	CH_3CCH	CH_3CHO	CH_2CHCN	c-CH_2OCH_2	CH_2CHOH
	C_6H	C_6H^-	HC_5N	C_2H_5SH		
8-atom	CH_3CHNH	CH_2CHCHO	NH_2CH_2CN	$HCOOCH_3$	CH_3COOH	CH_2OHCHO
	CH_3C_3N	$H_2CCCHCN$	HC_6H	H_2C_6	C_7H	
9-atom	CH_3CHCH_2	C_2H_5OH	CH_3OCH_3	C_2H_5CN	CH_3CONH_2	CH_3C_4H
	C_8H	C_8H^-	HC_7N	C_2H_5SH		
10-atom	CH_3COCH_3	CH_3CH_2CHO	$(CH_2OH)_2$	CH_3C_5N		
11-atom	C_2H_5OCHO	CH_3COOCH_3	CH_3C_6H	HC_9N		
12-atom	$C_2H_5OCH_3$	C_3H_7CN	C_6H_6			
13-atom	$HC_{11}N$					
>13-atom	C_{60}	C_{70}				

Analysis of the H_2 electronic transitions in many diffuse clouds shows that the fractional abundance of H_2, $f(H_2) = n(H_2)/n$ varies from very small values, $\sim 10^{-5}$, to much larger values, ~0.3, over a very small range of A_V and provides significant insight into the formation and destruction processes of H_2. Since the radiative association of two H atoms to form H_2 is spin-forbidden, gas-phase routes to its formation must involve ions such as H^- and H^+, neither of which are abundant in diffuse clouds and, as a result, can form only insignificant amounts of H_2. The conclusion is that a third body, namely a dust grain, provides the means by which excess energy is removed from the recombination of two hydrogen atoms on its surface. Simple models of this process show that the physical properties of the gas and grains are sufficient to sustain a low fractional abundance, around $10^{-5} - 10^{-4}$ in gas at very small extinctions, on the order of 0.1 magnitudes, irradiated by the average interstellar radiation field.

The steep rise in $f(H_2)$ as a function of A_V is due to the fact that H_2 is not photodissociated by continuum photons but through the absorption of FUV line photons which excite the molecules into the Lyman and Werner bands, with a significant fraction of the de-excitations, ~0.15, leading to the vibrational continuum of the ground electronic state. Since these line photons are removed through the absorption process, the intensity of photons at these specific wavelengths decreases rapidly as flux is removed from the photon field much faster than the continuum photons which are predominately absorbed by dust grains—H_2 is said to self-shield—and, as a result, the photodissociation rate of H_2 is several orders of magnitude less than that of other molecules at $A_V > 0.1$ magnitudes.

Interestingly, Schilke *et al* (2014) have detected absorption from $^{36}ArH^+$ and $^{38}ArH^+$ toward several lines of sight through diffuse interstellar material. By comparing with a variety of low density gas tracers, they find that ArH^+ is an

excellent tracer of atomic hydrogen gas, in particular, it is a unique tracer of gas in which the molecular hydrogen fraction is $10^{-4} - 10^{-3}$. Argon cannot be ionized by the relatively low energy photons in the ISM but by high energy cosmic ray particles. Subsequently Ar^+ reacts with H_2 to form ArH^+. It is destroyed mainly through exothermic proton transfer reaction with H_2 as its dissociative recombination reaction with electrons is slow.

1.1.2. Dark interstellar clouds. Dark clouds are so-called because they are opaque to visible and UV radiation and hence 'black out' background star fields. They have number densities $n \sim 10^4 - 10^6\,\mathrm{cm}^{-3}$. The exclusion of UV photons leads to a number of important consequences for the gas. Photodissociation and photoionization are negligible so that, except for edge effects, both the gas temperature, ~10 K, and the fractional ionization, $f(e) \sim 10^{-7} - 10^{-8}$, are much reduced from their values in diffuse clouds.

The lack of UV photons enables essentially all atomic hydrogen atoms that are converted to molecular form on grain surfaces to survive. The fractional abundance of the residual atomic hydrogen, which is hard to detect in these clouds, is likely to be $\sim 10^{-4} - 10^{-6}$. Molecules in these clouds are mostly detected through millimetre and submillimetre observations of rotational emission lines which are sensitive down to fractional abundances of $\sim 10^{-12}$ depending on the species. To date, over 60 molecules have been detected in these objects and used to show that dark clouds typically have masses ~ 1–500 $M_\odot$ and sizes ~1–5 pc. High spectral resolution observations show that the line widths in many dark clouds are consistent with thermal motion plus a degree of subsonic turbulence with some clouds showing evidence of infall onto a protostar—a newly forming star. Given the low efficiency of star formation in the Milky Way Galaxy, dark interstellar clouds are likely to form one or two low-mass stars, that is, stars with masses on the order of a solar mass.

The molecular composition of dark clouds is characterised by two observational results. One is that many of the polyatomic species are carbon-chain molecules, such as cyanopolyynes, $HC_{2n+1}N$ (n = 0–5), cummulenes H_2C_n (n = 2–4), polycarbon sulphides C_nS (n = 2–4) and polycarbon monoxides C_nO (n = 2–3), $C_{2n+1}N$ (n = 1, 2), HC_n (n = 2–8), as well as carbon-chain anions C_4H^-, C_6H^- and C_8H^-, perhaps surprising observations given the extremely large abundance of hydrogen relative to carbon in interstellar clouds.

The second observation is that many molecules contain enormous enrichments of deuterium, that is the abundance ratio of a deuterated molecule, XD, compared to its hydrogenated analogue, XH, is much larger than that of the cosmic abundance ratio of D to H, $\sim 2 \times 10^{-5}$. In these cold, dark clouds, deuterated fractions of up to 0.3 of have been detected (in HDCO). Indeed doubly and triply-deuterated molecules, such as D_2CO and ND_3, have been observed (Lis *et al* 2002, Parise *et al* 2006, Roberts and Millar 2007). The abundance ratio of ND_3 to NH_3 is about 10^{-3}, some 11 orders of magnitude greater than the statistical, cosmic ratio, $(D/H)^3 \sim 10^{-14}$. This enhancement process, called fractionation, is a kinetic effect driven by zero-point energy differences, and allows deuterated species to be very important probes of low temperature physics and chemistry in dark clouds as we will discuss further in section 2.3.

1.1.3. Protoplanetary disks. The gravitational collapse of interstellar gas in a dark cloud to form a solar-type star proceeds through a protoplanetary disk (PPD), a thin, rotating, flattened structure which acts as an engine that allows mass to accrete on to a central object whilst dissipating angular momentum through turbulent viscosity. A comprehensive model of the physics and chemistry within such a PPD is impossible to make at the present time and here we discuss how one can derive a basic structure for the disk that may be used in chemical kinetic modelling and as a basis of further, more advanced, models. The model is self-consistent in that it adopts hydrostatic equilibrium in the vertical direction and uses local thermal balance to determine the gas temperature. The temperature of the dust grains is calculated separately and, although there are large regions within the disk where the dust and gas are in thermal equilibrium, there are significant regions in which the dust is much cooler than the gas.

Hydrostatic equilibrium in the vertical direction assuming cylindrical, (r, z), coordinates is given by:

$$\frac{\mathrm{d}P}{\mathrm{d}z} = -\frac{\rho G M_* z}{(r^2 + z^2)^{3/2}} \tag{1}$$

where P is the pressure ($P = \rho \mathrm{kT}/\bar{m}$), with ρ, T and $\bar{m}$ the density, temperature, and mean molecular mass of the gas and M_* is the mass of the central protostar. It is useful to write the density distribution in terms of the surface density at a radial distance r, $\Sigma(r)$, defined as

$$\Sigma(r) = 2\int_0^{z_\infty} \rho(r, z)\mathrm{d}z \tag{2}$$

where z_∞ represents the surface of the desk and is often taken to be the value of z at which the local density matches that of the ambient molecular material in which the disk is embedded. The radial distribution of matter is found by equating the gravitational energy released by the accreting mass to the thermal heating via viscous dissipation in the disk midplane (Lynden-Bell *et al* 1974, Pringle 1981) at radius r, so that:

$$\frac{9}{4}\Sigma\alpha c_{s0}^2 \Omega_\mathrm{K}(r) = \frac{3GM_*\dot{M}}{4\pi r^3}\left[1 - \left(\frac{R_*}{r}\right)^{1/2}\right] \tag{3}$$

where c_{s0} and $\Omega_\mathrm{K}(r)$ are the sound speed in the disk midplane, $(kT_0/\bar{m})^{1/2}$, and Keplerian frequency, $(GM_*/r^3)^{1/2}$, respectively, R_* is the stellar radius, $\dot{M}$ is the mass accretion rate, and α is a viscous parameter related to the turbulent viscosity by $\nu = \alpha c_s H$, where H is the scale-height of the disk, $H = c_s/\Omega_\mathrm{K}$.

The radial infall velocity is given by:

$$v(r) = -\dot{M}/2\pi r\Sigma(r) \tag{4}$$

with the accretion timescale, $t_\mathrm{acc} \sim r/v(r)$.

In the models described later (section 2.2), we assume $\alpha = 0.01$, $\dot{M} = 10^{-8} M_\odot$ yr^{-1}, $M_* = 0.5 M_\odot$, $R_* = 2R_\odot$, $T_* = 4000$ K and the luminosity $L = 0.87 L_\odot$, representative of a T Tauri star, and which corresponds to a disk mass of

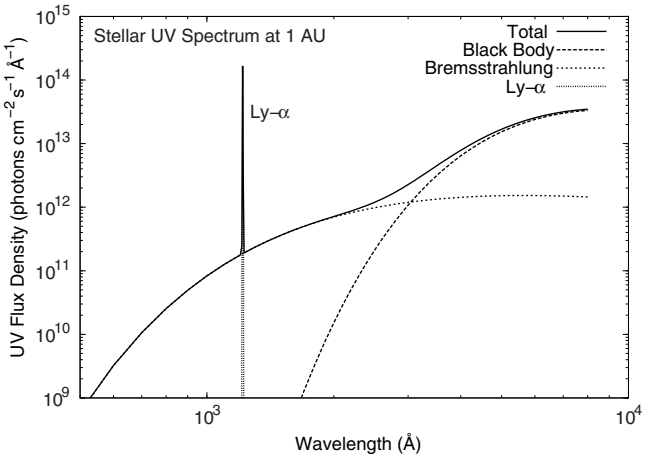

Figure 1. The ultraviolet spectrum of a typical T Tauri star (from Nomura and Millar (2005) © ESO).

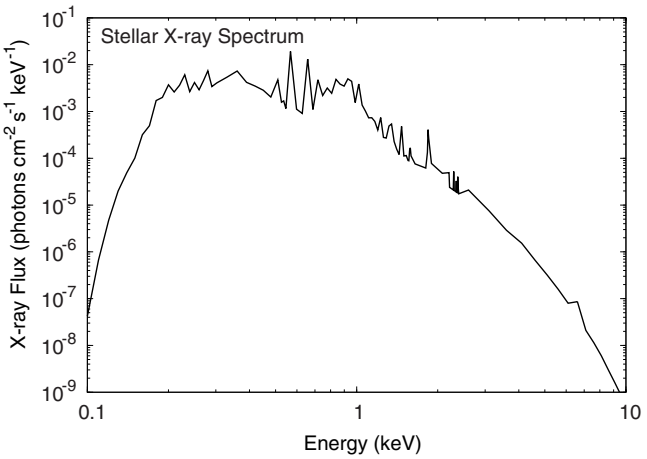

Figure 2. Calculated x-ray spectrum of a T Tauri star taking into account elemental extinction and Compton scattering. The flux is calculated for a T Tauri star at a distance of 56 pc (from Nomura *et al* (2007) © 2007. The American Astronomical Society.).

$0.024M_{\odot}$ between r = 0.01 and 300 AU (1 AU = average Earth–Sun distance, $\sim 1.5 \times 10^{13}$ cm). The accretion velocity is around a few tens of cm s^{-1} so that it takes more than one million years for material to move from the outer edges of the disk, at 300 AU, to the central protostar.

The FUV radiation field, which is important for photoionization, photodissociation and grain heating has four components: blackbody emission at the star's effective temperature, T_{*}, intense Lyman alpha emission over a narrow bandwidth, typically 2 Å, optically thin bremsstrahlung emission, and the interstellar radiation field, with a total luminosity of $L_{\rm UV} = 10^{31}$ ergs s^{-1}. Figure 1 from Nomura and Millar (2005) shows the radiation field for a typical low-mass protostar. In addition to FUV radiation, ionization is also provided by stellar x-ray photons, cosmic ray particles and radioactive decay, primarily from the decay of ^{26}Al to ^{26}Mg—an excess of ^{26}Mg found in the Allende meteorite Lee *et al* (1977) shows that ^{26}Al was present in the early Solar System and thus is likely to be present in protostellar disks.

The x-ray flux of T Tauri stars can be significant, $L_X \sim 10^{30}$ ergs s^{-1}, and a typical spectrum, calculated using a two-temperature thermal model with extinction due to ionization of the elements and Compton scattering by hydrogen, is shown in figure 2. Although the flux of x-rays is less than that of FUV radiation, the higher penetration power of x-ray allows them to penetrate to the disk midplane beyond a radius of 10 AU. Cosmic ray particles and radioactive decay provide a low level of ionization in those regions of the disk that are optically thick to the stellar FUV and x-ray radiation.

Since the gas and grain temperatures have an important influence on the chemistry, for example, controlling freeze-out of the gas to the grains and thermal desorption from the grains, it is important to calculate the thermal balance of both gas and dust as accurately as possible. Woods and Willacy (2009) provide a detailed list of important processes—in essence, energy is input to the PPD through FUV and x-ray radiation and is lost to the system by fine structure transitions of atoms and atomic ions, primarily in the surface layers of the disk, and vibrational and rotational transitions in the molecular gas, as well as through infrared continuum emission from the grains. At high densities the gas and grain temperatures are coupled through collisions but this breaks down in the less dense upper regions of the disk where the gas temperature can reach 4000 K while the grain temperature is typically an order of magnitude less. Figure 3 shows the gas and grain temperatures, density, FUV and x-ray fluxes for the disk model parameters listed above (Walsh *et al* 2012). One sees that the density ranges over some 10 orders of magnitude and in the hot inner disk, inside 1 AU, can reach values where three-body reactions become important.

It is worth noting at this point that the combination of high density and cold gas and dust throughout a sizeable fraction of the disk will lead to a freeze-out of gas onto the dust grains, forming molecular ice mantles. Such freeze-out occurs on a timescale t(yr) $\sim 3 \times 10^9/n$ (cm^{-3}), that is, less than 10^4 yr, much less than the typical accretion time-scale mentioned above. Thus we expect that in the disk midplane, far from the protostar, essentially all gas-phase species, with the exception of hydrogen, helium and related species, will have negligible abundance. Thus, the initial state for subsequent chemistry as these dust grains move radially inwards is dominated by the composition of the ice and its desorption kinetics as it is impacted by FUV, x-ray and cosmic ray particles on its journey. Given that these molecular ices may survive for more than 10^5 year in a disk before removal, it is also important to ascertain whether surface and/or volume chemistry could occur and alter the ice composition before mantle removal.

1.1.4. Hot molecular cores. While PPDs are known to be intimately connected with the formation of low mass stars like our Sun, there is no generally accepted theory for the formation of massive stars, that is, stars with masses greater than about 8–10$M_{\odot}$. The basic problem is that if stars form from the gravitational collapse of cloud material, radiation pressure from the ever-growing protostar can halt the infall process before stars with large masses can be made.

Observations of the formation of massive stars are surprisingly difficult to make even though their luminosities can be $10^4 - 10^5$ times larger than their lower-mass counterparts. This

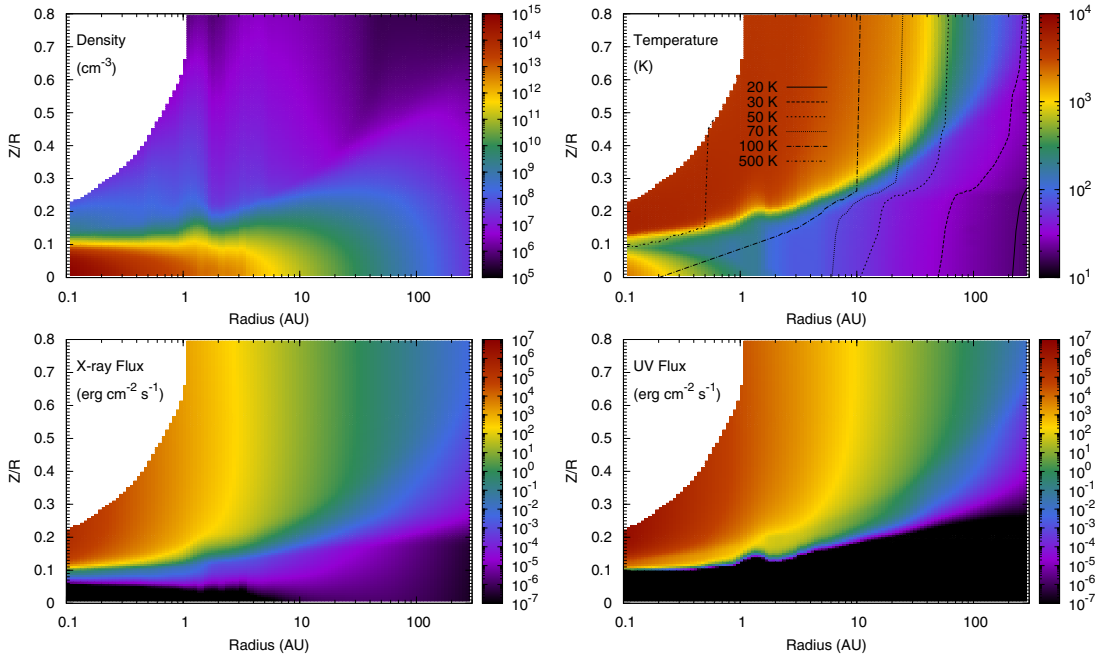

Figure 3. Neutral density (cm^{-3}), temperature (K), x-ray and UV fluxes (erg cm^{-2} s^{-1}) for a typical low mass T Tauri star (from Walsh *et al* (2012) © 2012. The American Astronomical Society.).

difficulty is due to the fact that the time-scale for the onset of nuclear fusion is a strong function of stellar mass, so that massive stars form rapidly, in around 5×10^4 yr compared to 10^7 yr for a solar-mass star, are very energetic, and disperse their natal material within a few hundred thousand years. As a result, massive stars are more difficult to catch in the star-formation phase and are, in addition, much less numerous than low-mass stars with the result that high-mass, star-forming regions are generally much more distant, by factors of 20–100, than those forming low-mass stars, with a concommitant loss of spatially resolved information.

Massive stars do, however, have several advantages for the molecular astrophysicist. Because of their mass they generally form out of more massive interstellar clouds, perhaps up to $10^3 - 10^4 M_\odot$, and because of their large luminosities they can heat large masses of dense gas to a very high temperature, at least by interstellar standards, ~100–300 K. Although this gas is dispersed on timescales of 10^4 years or so, it contains a very rich mix of molecules evaporated from ices, as well as those processed in the gas phase, that are readily observed with radio telescopes.

Because it is difficult for some massive stars to heat a significant volume of high-density, molecular gas in competition with efficient cooling through molecular line emission, the sizes of these hot molecular cores (HMCs) are generally small, ~0.01–0.1 pc, compared to the larger, colder molecular clouds (or envelopes), which can be 10–100 times larger, in which they are embedded. The molecular composition of HMCs is significantly different to that of cold, dark interstellar clouds and it is this composition that points unambiguously to the role of heterogeneous chemistry. In particular, HMCs contain large abundances of fully hydrogenated molecules such as NH_3, CH_4, H_2S, CH_3OH, C_2H_5OH and so on, with fractional abundances that are enhanced by factors of $10^3 - 10^6$ over those in dark clouds. In these latter objects, abundances are determined, in the main, by gas-phase chemistry. Although the higher temperatures in HMCs do allow for some gas-phase reactions to proceed more rapidly, this cannot account for all such enhanced abundances. In addition, fractionation of deuterium in HMCs, that is, the abundance ratio of D/H in molecules, is typically 10–100 times the cosmic D/H ratio, although smaller than the enhancements of $10^4 - 10^5$ seen in dark clouds. As will be discussed in section 1.3, fractionation is not efficient at the temperatures of HMCs and the observed abundances are, rather, indicative of cold chemistry, at ~20–50 K. This, together with the large abundances of hydrogenated molecules, can be explained if the molecules detected in the hot gas phase through rotational line emission are formed as cold ice mantles on dust grains, mantles that are evaporated readily by radiation from a newly-formed, massive star. Simple molecules such as H_2O and CH_4 that evaporate as parents can, of course, take part in subsequent gas-phase chemistry to form daughter molecules, some of which can be quite complex, for example methyl ethyl ether. Since the abundance of such parent and daughter molecules evolve rapidly with time, observations of molecules have the potential to determine time scales in the formation of massive stars as well as to act as effective probes of the cold ice chemistry, a chemistry which may have been occurring for perhaps one million years before the onset of massive star formation returned ice mantles to the gas phase.

Although relatively small, HMCs are very dense by normal standards for molecular clouds, $n(H_2) \sim 10^7 - 10^9$ cm^{-3}, have masses of a few thousand solar masses and very large column densities, $N(H_2) \sim 10^{24} - 10^{25}$ cm^{-2}, compared to 10^{22} cm^{-2} in dark clouds, and relatively small electron fractions, on the order of $10^{-10} - 10^{-11}$. Thus, although physically small, this combination of density, temperature, mass and large

abundances of complex organic molecules means that the sub-millimetre spectra of HMCs are very bright and line rich, indeed observed spectra can be so line rich that line blending causes significant difficulty in identifying specific transitions and molecules.

1.1.5. Giant molecular clouds. Although individual molecular clouds do exist, many of the types of environment discussed above can be found within much larger, coherent structures called Giant Molecular Clouds (GMCs). These GMCs can be very large, perhaps several hundred pc in size, and form, with the possible exception of the black hole at the Galactic Centre, the most massive objects in the Milky Way, with typical masses ranging from $10^5-10^6 M_\odot$. Star formation is a very active process within GMCs, some 3–5% of their mass will eventually end up in new stars, and phenomena associated with star formation—photoionization, stellar winds, supernovae—return significant energy to the molecular gas and can alter appreciably physical and chemical characteristics through, for example, the propagation of hydrodynamic and MHD shocks. Such shock waves can drive a significantly different chemistry in post-shock gas than that described here-to-fore. Typically, shock waves both compress and heat the gas, often to several thousand degrees, and can return heavy atoms, such as Si, to the gas due to sputtering from dust grains. At such high temperatures, reactions of neutral species with H and H_2 become efficient and can lead to abundances much different from colder chemistries. The topic of shock chemistry, important in some specific regions, is discussed briefly in section 2.6.

The role of magnetic fields and its coupling to charged particles is particularly important in star formation since they control the ability of gas to undergo gravitational collapse. If the ionization level is high, then collisions between ions and the neutrals couple the neutrals to the magnetic field and create a magnetic pressure which is able to resist collapse. In dense cores, however, the ionization fraction is low, less than 10^{-7}, thereby allowing the neutral gas to decouple from the field and collapse. This process of ambipolar diffusion, which has long been viewed as the standard model for star formation, accounts naturally for the low efficiency of star formation. Since it is a slow process, taking around 10 Myr, molecular clouds are long-lived objects. Whether a particular dense core in a GMC will collapse can be determined by a consideration of its mass-to-flux ratio in comparison to the critical ratio which separates out material which can collapse (supercritical) from that which cannot (subcritical, for example, the molecular cloud envelope).

This theory of star formation can be probed through measurement of the magnetic field strength through observations of Zeeman splitting in emission lines from molecules such as OH and CN. These give the line-of-sight component, B_z, of the magnetic field while linear polarization measurements of the thermal continuum emission from dust grains give the field in the plane of the sky. The ionisation fraction cannot be measured directly in clouds but can be estimated from measurements of deuterium fractionation, such as the DCO^+/HCO^+ abundance ratio (see section 2.3). We note though that the use of molecular emission lines, which are sensitive to local densities since they are excited by collisions, means that the measurements necessary to be made may not always sample the same volume of the cloud.

Crutcher *et al* (2009) have performed Zeeman observations of OH toward four molecular cloud cores and their surrounding envelopes and find that the mass-to-flux-ratio in the cores are less than in their corresponding envelopes, the opposite behaviour to that predicted by the ambipolar diffusion model of star formation. This suggests that an alternative theory of star formation may be required. One recent suggestion is that molecular clouds form from the collision of turbulent supersonic flows. Only those, a minority of clouds, which are gravitationally bound collapse rapidly in a free-fall time (section 1.3.3) to form stars; most clouds dissipate thereby keeping the overall efficiency of star formation low, as required. Crutcher (2012) has recently reviewed the role of magnetic fields in molecular clouds.

1.2. Interstellar dust

The presence of dust grains has been known for more than a century and measurements of absorption and scattering of star light from ultraviolet to submillimetre wavelengths have led to a consensus that the grains are non-spherical, sub-micron sized particles composed of silicates and carbonaceous materials. These are most likely formed in the cooling gas following supernovae explosions as well as in the atmospheres of late-type, cool stars which can be either oxygen-rich, with the abundance of O greater than that of C (O/C > 1) forming silicates, or carbon-rich, with the abundance of C greater than that of O (O/C < 1), forming carbonaceous grains.

Fitting the observed behaviour of extinction and polarization as a function of wavelength gives a non-unique description of grain size, shape, porosity, and composition although size distributions based on a power-law size distribution of spherical grains or a continuous size distribution of ellipsoids are widely used in the literature. While such dust grains likely remain bare in the general interstellar medium, in cold, denser regions they can be covered by ice mantles. The infrared spectra of such grains, such as that shown in figure 4 (Gibb *et al* 2000), can be used to identify the most common molecular components of the ice—H_2O, CO, CH_3OH, CO_2—and their abundances relative to hydrogen. Such observations are sensitive enough to trace molecules down to fractional abundances (relative to hydrogen), of about $10^{-6} - 10^{-7}$, that is 1–0.1% of that of water ice, the dominant component of interstellar ices.

Finally, a number of infrared emission bands have been detected in regions in which grains are irradiated by ultraviolet photons. These bands have been identified with the stretching and bending modes in polycyclic aromatic hydrocarbon (PAHs) and, although no individual PAH has yet been identified in space, the band intensities are consistent with some 10–20% of the total cosmic carbon abundance being in this form. Detailed modelling of the continuous emission seen at 2–10 μm indicates that the PAHs must be small, ∼30–100 carbon atoms. Figure 5 shows an example of the types of PAH molecules that are thought to be present in the interstellar medium together with the 3–20 μm

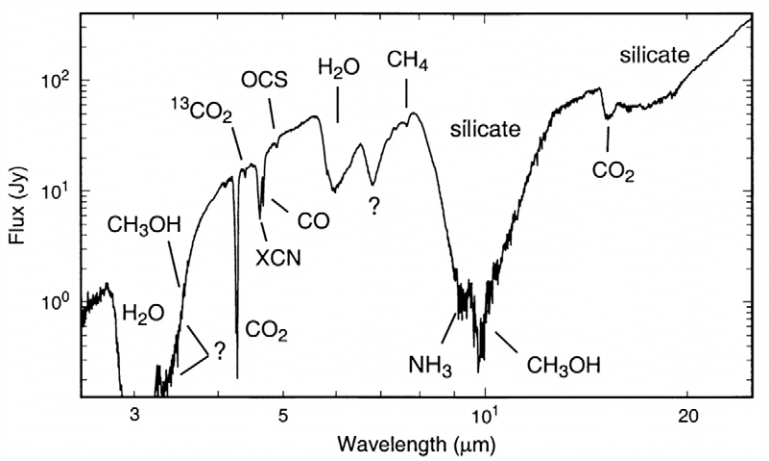

Figure 4. Infrared spectrum of the deeply embedded protostar W33A showing a variety of absorption bands due to solid state molecules frozen on to the surfaces of silicate dust grains (from Gibb *et al* (2000) © 2000. The American Astronomical Society.).

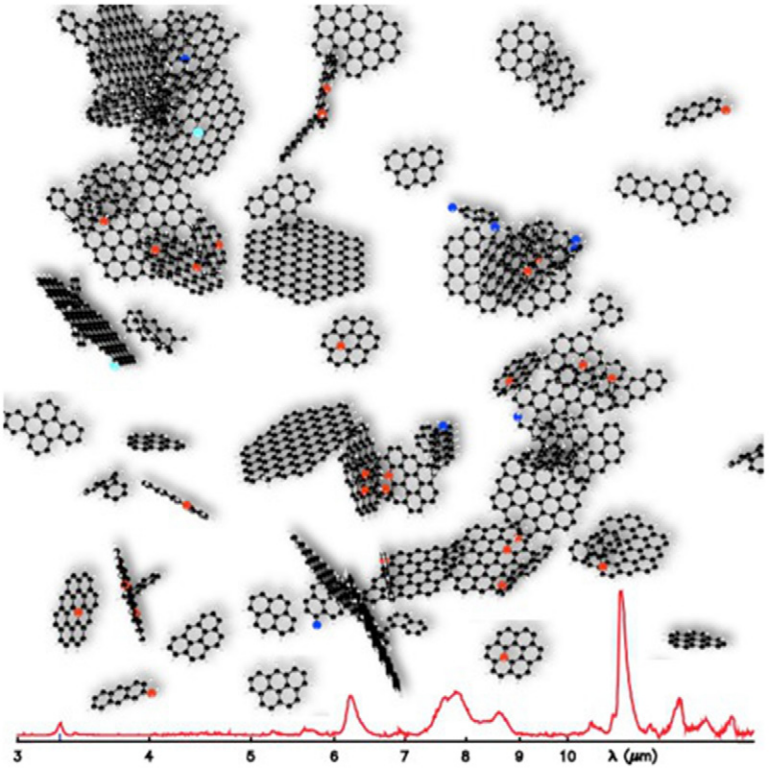

Figure 5. A selection of the types of PAH molecules though to be present in the interstellar medium. Colour coding: hydrogen (white), carbon (black), nitrogen(red), oxygen (blue), magnesium (cyan).The spectrum is a typical 3–20 μm interstellar PAH emission spectrum. Figure courtesy of Christian Boersma and Lou Allamandola.

spectrum that they give rise to. The origin of these PAHs is unknown but it is likely that they are formed in cool, carbon-rich stars. However, none has been detected in such environments since they lack the source of UV photons that drives the infrared fluorescence. Hence only the most radiation stable are able to survive for periods of 10^7-10^8 years, needed to populate the general interstellar medium (ISM) with dust.

Although no single PAH has been identified, there is evidence for the presence of specific molecules containing tens of carbon atoms, namely the fullerenes C_{60} and C_{70}. Cami *et al* (2010) used the Spitzer Space Telescope to detect several infrared emission bands in the 7–19 μm wavelength range from both molecules in the young planetary nebula Tc 1. Subsequently, C_{60} has been detected in a number of different objects including planetary nebulae in both the Milky Way and Large Magellanic Cloud galaxies, in late-type stars, in the transition phase between such stars and planetary nebulae and in some young, star-forming objects. Although seen in a variety of sources, the fullerenes are not common, detected in only around 3% of carbon-rich planetary nebulae searched with Spitzer.

Astronomers use magnitudes to measure brightness with a magnitude difference of five between two objects equal to a brightness ratio of 100. Studies of lines-of-sight to nearby bright stars show that there is a relationship between the column density of hydrogen nuclei, N_H, and the visual extinction, A_V, (absorption + scattering), due to the dust grains implying that the gas and dust are generally well mixed in the ISM. In particular, the ratio is given by $A_V/N_H = 5.1 \times 10^{-22}$ magnitudes cm^2 per H nucleon (Ratchford *et al* 2009). For atomic hydrogen gas of average density 1 cm^{-3} over a path length of 1 kpc ($= 3.086 \times 10^{21}$ cm) this gives rise to 1.6 magnitudes of extinction in the V band (550 mm). In terms of optical depth $A_V = 1.086\tau_V$.

Observational studies of the relationship between the gas and dust have shown that the dust coincides spatially with the gas with a mass ratio of about 1% and an average cross-section per unit volume $< \pi a^2 n_d > \sim 6 \times 10^{-22} n$ cm^{-1}, where the grains are assumed to be spherical, radius a, and number density n_d per unit volume, and n is the number of hydrogen nuclei per unit volume, with $n = n(H) + 2n(H_2)$.

As well as providing extinction, dust grains also remove heavy elements—C, N, O, Mg, Si, Fe, etc—from the gas phase, so-called elemental depletion, thereby ensuring that not all of an element's cosmic abundance is available for molecule formation. Although the presence of dust reduces the absolute abundances of the elements from which molecules are formed in the gas-phase, grain surfaces also provide an important environment on which chemical species can meet and react. The long periods of time in which an atom, radical or molecule can spend on a dust grain, perhaps in excess of one million years, makes surface chemistry viable even if reaction rates are low due to the very low temperatures, 10–20 K, of the dust particles. Most importantly, grain surfaces provide an extremely efficient environment for the formation of H_2, a subject to which we return later in this article.

The temperature of dust grains in the ISM is determined by the balance between heating, dominated by the absorption of UV photons in regions of low extinction, and collisions with gas and cooling by thermal emission. In regions with densities less than about 10^6 cm^{-3}, collisions are too slow to equilibrate the gas and dust temperatures, and as a result, the grain temperatures can be very low, ∼6–10 K in a dark cloud core, to ∼ 15 K in cloud edges, to ∼20–25 K in diffuse clouds.

1.3. Time scales

At this point, it is worth considering some typical time scales that are relevant in interstellar chemistry.

1.3.1. Chemical time scale. We can define a chemical time scale from the reaction of neutral species A with a partner X, as:

$$t_r = [kn(X)]^{-1} \text{ s} \quad (5)$$

where $n(X)$ is the abundance (concentration) of X per unit volume and k is the rate coefficient. For ion-neutral reactions, $k \sim 10^{-9}$ cm^3 s^{-1}; for important, exothermic neutral–neutral reactions, $k \sim 10^{-10}$–10^{-12} cm^3 s^{-1}. Thus, for a dark cloud, if the colliding partner is H_2, the most abundant interstellar molecule, then $t_r \sim (10^{-9} \times 10^4)^{-1} = 10^5$ s, around 1 d for reaction with an ion, and about 10–100 d for reaction with a neutral at a density $n(H_2) = 10^4$ cm^{-3}. Reactions of A with other atoms and molecules occur on a time scale at least 100 times longer. Thus, since collisions with H_2 also de-excite molecules, radiative and collisional decay means that it is generally the case that reactions in the interstellar medium involve species in their ground electronic and vibrational states. In diffuse clouds, photoprocesses are important with $t_r \sim 10^{10}s \sim 300$ yr for the average interstellar radiation field. In dense clouds, ionization is provided by high energy cosmic ray protons on a time scale of 10^5 yr.

1.3.2. Grain accretion time scale. Observations of the interstellar extinction of starlight allows one to estimate the surface area of dust grains per unit volume and thus the time-scale for a gas-phase species to collide with an interstellar dust grain. Observations shows that gas and dust in the Milky Way are extremely well mixed, with a fairly constant gas-to-dust mass ratio of 100:1. For the grains responsible for the visual extinction in the interstellar medium, with sizes ∼0.1 μm, the number of dust grains per unit volume, $n_d \sim 10^{-12}n$, where n is the density of H nucleons. In diffuse clouds, grains of size ∼ 0.01 μm provide extinction in the ultraviolet, larger in magnitude to that in the visible part of the spectrum, and have about 10 times the surface area of the larger grains. In cold dense clouds, these small grains are likely removed by coagulation or conglomeration processes which produce fewer, larger particles with a reduced surface area overall. Using these values we can derive an accretion time scale for species A to freeze-out on the surface of dust as:

$$t_{ac,d} = [\pi a^2 n_d v_A]^{-1} \text{ s} \quad (6)$$

where v_A is the velocity of A relative to the dust grain, or $t_{ac,d} \sim 3 \times 10^9/n$ yr where n is the number of hydrogen nucleons cm^{-3}. Thus one sees that accretion and ice mantle formation can be a significant, in fact, dominant process in cold, dark clouds and in the cold midplanes of protoplanetary disks.

1.3.3. Dynamical time scales. Since there is a variety of physical processes that drive dynamics in molecular clouds, there is a variety of time scales that can be important. Here we mention only one.

The free-fall time, t_{ff}, is a crude, miminum measure of the time it takes for a molecular cloud to collapse under the effect of its self-gravity to form a star. If we assume that the cloud is homogeneous with initial hydrogen nucleon density n_0 cm^{-3}, then the free-fall time scale is given by $t_{ff} = (3\pi/32G\rho_0)^{1/2}$, that is, t_{ff} (in years) is $\sim 5 \times 10^7/n_0^{0.5}$. This time-scale is, in fact, too short, perhaps by an order of magnitude, when compared to the observed efficiency of star formation, not surprising since its derivation neglects internal pressures, such as turbulence, as well as rotational and magnetic pressures, that oppose gravitational collapse.

We conclude this section by noting that there are situations in interstellar clouds in which gas-phase chemical reactions, grain accretion, and dynamics will occur on similar times

scales and that these lead to a complex, non-linear interplay between physics and chemistry which must be expressed via the specific chemical kinetic and dynamical equations. Once expressed, these equations must be solved in a self-consistent manner in order to understand both chemical evolution and the emission properties of gas in molecular clouds. For the most part, this holistic description is still beyond our reach.

2. Basic chemistry

In this section I shall review the reactions that turn atomic gas into molecular gas in interstellar clouds. We refer to our discussion in section 1.1.1 in which it was pointed out that H_2 forms through the reaction of two hydrogen atoms on the surface of a dust grain. In this section, however, we concentrate on the basic gas-phase chemistry that turns atoms and atomic ions into molecules. We begin with diffuse clouds in which O and N are in neutral form and the other common elements are photoionized by the UV radiation field (see table 1). In all cases where particular rate coefficients are given explicit values, the data are taken from the Rate12 version of the UMIST Database for Astrochemistry at URL www.udfa.net (McElroy *et al* 2013).

2.1. Hydride formation

The dominant form of carbon in diffuse clouds, C^+, does not react with H_2 because of a large endothermicity, but is able form CH_2^+ through an inefficient radiative association:

$$C^+ + H_2 \longrightarrow CH_2^+ + h\nu \quad k = 2\,10^{-16}(T/300)^{-1.3}e^{-23/T}cm^3\,s^{-1} \tag{7}$$

that is, only 1 in 10^6 collisions of C^+ with H_2 lead to CH_2^+. In diffuse clouds the most abundant, chemically active species are H, H_2 and e^-. CH_2^+ can undergo a number of competing reactions the most important of which are:

$$CH_2^+ + H_2 \longrightarrow CH_3^+ + H \quad k = 1.6\,10^{-9}\,cm^3\,s^{-1} \tag{8}$$

$$CH_2^+ + e^- \longrightarrow C + H_2 \quad k = 7.68\,10^{-8}(T/300)^{-0.6}\,cm^3\,s^{-1} \tag{9}$$

$$CH_2^+ + e^- \longrightarrow C + H + H \quad k = 4.03\,10^{-7}(T/300)^{-0.6}\,cm^3\,s^{-1} \tag{10}$$

$$CH_2^+ + e^- \longrightarrow CH + H \quad k = 1.60\,10^{-7}(T/300)^{-0.6}\,cm^3\,s^{-1}. \tag{11}$$

Since the abundance of H_2 is $\sim 10^4$ that of e^- (= the abundance of C^+), CH_2^+, once formed, reacts quickly with H_2 to form CH_3^+. The methyl ion does not react with H_2 as the reaction to form CH_4^+ is endoergic but it can undergo radiative association to form CH_5^+:

$$CH_3^+ + H_2 \longrightarrow CH_5^+ + h\nu \quad k = 3.92\,10^{-16}(T/300)^{-2.3}e^{-21.3/T}\ cm^3\,s^{-1} \tag{12}$$

Since this reaction is relatively slow, dissociative recombination of CH_3^+ dominates its loss, producing simple hydride radicals CH and CH_2 (Mitchell 1990):

$$CH_3^+ + e^- \longrightarrow CH + H_2 \quad k = 1.95\,10^{-7}(T/300)^{-0.5}\,cm^3\,s^{-1} \tag{13}$$

$$CH_3^+ + e^- \longrightarrow C + H + H \quad k = 2.00\,10^{-7}(T/300)^{-0.4}\,cm^3\,s^{-1} \tag{14}$$

$$CH_3^+ + e^- \longrightarrow CH_2 + H \quad k = 7.75\,10^{-8}(T/300)^{-0.5}\,cm^3\,s^{-1}. \tag{15}$$

The formation of simple hydride radicals allows for other molecules to form, for example:

$$C^+ + CH_2 \longrightarrow C_2H^+ + H \quad k = 5.20\,10^{-10}\,cm^3\,s^{-1} \tag{16}$$

$$O + CH_2 \longrightarrow CO + H + H \quad k = 1.33\,10^{-10}\,cm^3\,s^{-1} \tag{17}$$

$$O + CH \longrightarrow CO + H \quad k = 6.02\,10^{-11}(T/300)^{-0.1}\,cm^3\,s^{-1}. \tag{18}$$

These simple formation routes, when coupled with fast destruction of neutrals by UV photons in diffuse clouds, typically lead to fractional abundances of carbon hydrides and CO around 10^{-8} and 10^{-6}, respectively, to that of hydrogen. Thus at most 1% of carbon is processed into molecules in diffuse clouds. Since O is neutral in diffuse clouds and the reaction of O with H_2 is endoergic, oxygen hydrides form by a different process, one that is sensitive to the gas kinetic temperature and to the rate of cosmic-ray ionization.

The passage of cosmic rays through interstellar gas leads to ionization, although only that concerned with the most common species H, H_2 and He, plays a significant role (recall that these species cannot be ionized by the UV radiation field). The key to oxygen chemistry is the fact that the ionization potential of O is only slightly larger than that of H, in fact the difference is equivalent to a temperature $\Delta E/k = 224.3$ K. Thus, if diffuse clouds are warm enough, greater than about 50–60 K, the energy barrier can be overcome, so that:

$$O + H^+ \longrightarrow O^+ + H \quad k = 6.86\,10^{-10}(T/300)^{-0.26}e^{-224.3/T}\ cm^3\,s^{-1} \tag{19}$$

becomes an important loss route for H^+ rather than the slow radiative recombination with electrons.

Once formed, O^+ reacts rapidly with H_2 in a series of exoergic reactions to form H_3O^+ which recombines with electrons to form OH and H_2O:

$$O^+ + H_2 \longrightarrow OH^+ + H \quad k = 1.70\,10^{-9}\,cm^3\,s^{-1} \tag{20}$$

$$OH^+ + H_2 \longrightarrow H_2O^+ + H \quad k = 1.01\,10^{-9}\,cm^3\,s^{-1} \tag{21}$$

$$H_2O^+ + H_2 \longrightarrow H_3O^+ + H \quad k = 6.40\,10^{-10}\,cm^3\,s^{-1} \tag{22}$$

in competition with dissociative recombination of the intermediate ions to form O and OH. The barrier in (19) and photodissociation again restrict abundances—typically OH is more abundant than CH in warm diffuse clouds but the predicted fractional abundance of water is low, $\sim 10^{-8}$–10^{-9}.

Like oxygen, nitrogen is neutral in diffuse clouds but there is no easy way of ionizing it in these clouds. Instead, nitrogen

chemistry is driven by a series of neutral-neutral reactions such as:

$$N + OH \longrightarrow NO + H \quad k = 6.05\,10^{-11}(T/300)^{-0.23}e^{-14.9/T}\,cm^3\,s^{-1} \tag{23}$$

$$N + NO \longrightarrow N_2 + O \quad k = 3.38\,10^{-11}(T/300)^{-0.17}e^{2.8/T}\,cm^3\,s^{-1} \tag{24}$$

$$N + CN \longrightarrow N_2 + C \quad k = 1.00\,10^{-10}(T/300)^{0.18}\,cm^3\,s^{-1} \tag{25}$$

$$N + CH \longrightarrow CN + H \quad k = 1.66\,10^{-10}(T/300)^{-0.09}\,cm^3\,s^{-1} \tag{26}$$

$$N + CH_2 \longrightarrow HCN + H \quad k = 3.95\,10^{-11}(T/300)^{0.17}\,cm^3\,s^{-1} \tag{27}$$

and the abundance of N-bearing molecules is generally small, with CN and HCN having fractional abundances $\sim 10^{-8}$–10^{-9}. This combination of inefficient initiation of the chemistry, rapid dissociative recombination with electrons, due to high fractional ionization, and rapid photodissociation, means that molecules other than H_2 take up less than 1% of the elemental abundances and generally contain rather few, usually less than four, atoms.

In cold, dark clouds, however, molecule formation can be very efficient, in major part due to the lack of UV photons but also to the presence of a key interstellar ion H_3^+. In these objects all elements, with the exception of hydrogen which is largely in the form of H_2, begin as neutral atoms. The lack of UV photons has another important consequence for chemistry, namely that, only cosmic ray protons provide ionization. The much smaller ionization rates associated with this process, coupled with rapid dissociative recombination of molecular ions, leads to the result that the fractional ionization in dark clouds is low, $\sim 10^{-7}$–10^{-8} compared to 10^{-3}–10^{-4} in diffuse clouds.

In dark clouds, the basic driver for chemical synthesis of the hydrides, and indeed other molecules, is cosmic-ray ionization of the two most abundant gas-phase species, H_2 and He (the ionization of atomic hydrogen is not important here since its abundance is low):

$$H_2 + crp \longrightarrow H_2^+ + e^- \quad k = 1.20\,10^{-17}\,s^{-1} \tag{28}$$

$$He + crp \longrightarrow He^+ + e^- \quad k = 6.50\,10^{-18}\,s^{-1}. \tag{29}$$

The rates for cosmic-ray ionization quoted above are theoretical estimates based on assumptions about the interstellar flux of low-energy cosmic rays. Since these cosmic rays do not reach Earth we have only a poor handle on the ionization rates. Fortunately, spectrometers on large telescopes are now able to measure the absorption bands of H_3^+ in the near infrared and can lead to a more accurate estimate of the rate. Consider the case of H_3^+ in diffuse clouds where it is formed by cosmic ray ionization of H_2 and destroyed by dissociative recombination with electrons with rate coefficient k_e cm^3 s^{-1}. Assuming steady-state, a good approximation in these clouds, the ionization rate of H_2, ζ, is given by:

$$\zeta = k_e n(e) n(H_3^+)/n(H_2) \tag{30}$$

As stated in section 1.1.1, the electron abundance can be taken to be that of C^+, so that all quantities on the right-hand side can be measured either astronomically or in the laboratory. Indriolo and McCall (2012) have used this approach to determine ζ toward over 20 lines of sight and derive a mean value of 3.5×10^{-16} s^{-1}, somewhat larger than the value in (28) above. The variation of ζ toward different sight lines and a decrease in its value as the column density of hydrogen increases towards those typical of dense clouds indicates that magnetic fields may shield dense gas from low-energy cosmic ray protons.

He^+ is not reactive with H_2 (if it was, the H_2 abundance in molecular clouds would be significantly less) whilst the H_2^+ reacts immediately with H_2, that is within a day or so depending on density, to form H_3^+. Because of its low proton affinity (PA)—of all the abundant interstellar species only O_2 and N have PAs less than that of H_2—H_3^+ reacts with atoms. Thus carbon–hydrogen bonds are made via:

$$H_3^+ + C \longrightarrow CH^+ + H_2 \quad k = 2.00\,10^{-9}\,cm^3\,s^{-1} \tag{31}$$

with further exoergic hydrogen abstraction reactions with H_2 converting CH^+ to CH_3^+. As in diffuse clouds, CH_3^+ does not react with H_2 to form CH_4^+ but instead undergoes radiative association to form CH_5^+. The low electron abundance in dense clouds, however, means that dissociative recombination is much less important a loss for ions that react, even slowly with H_2, that is, a reaction of an ion and H_2 with a rate coefficient larger than 10^{-13} cm^3 s^{-1} would ensure that dissociative recombination, with a rate coefficient on the order of 10^{-6}–10^{-7} cm^3 s^{-1}, is unimportant.

In a similar fashion to C atoms, reaction of O with H_3^+ produces OH^+ which reacts with H_2 in a rapid sequence of reactions to form H_3O^+. Since neither CH_5^+ nor H_3O^+ react with H_2, dissociative recombination is now an important loss mechanism, producing reactive radicals such as CH_2, CH_3, O, and OH as well as the closed shell molecules, CH_4 and H_2O.

Reaction schemes similar to these occur for other elements, for example sulfur and chlorine. For nitrogen, however, the formation of N-H bonds in the gas phase is much less efficient because N cannot accept a proton from H_3^+ and cannot react with H_2 at very low temperatures. Ammonia, NH_3, is made in an sequence of reactions that require that N_2 is already present in the gas, via (24) and (25) above. Collisions of He^+ with N_2 produce kinetically excited N^+ and N atoms, with the N^+ ions having sufficient energy to overcome the small activation energy barrier of its reaction with ground state H_2, $\Delta E/k \sim 85$ K:

$$He^+ + N_2 \longrightarrow N^+ + N \quad k = 9.60\,10^{-10}\,cm^3\,s^{-1} \tag{32}$$

$$N^+ + H_2 \longrightarrow NH^+ + H \quad k = 1.00\,10^{-9}e^{-85/T}\,cm^3\,s^{-1}. \tag{33}$$

Once NH^+ forms, it undergoes a series of hydrogen abstraction reactions with H_2 to form NH_4^+, followed by dissociative recombination to form NH_3 and other N–H bearing radicals. A consequence of this very indirect synthesis is that ammonia abundances are relatively small, $\sim 10^{-9}$, in molecular clouds, at least those in which gas-phase chemistry dominates.

Once small radicals and quasi-stable ions, i.e. those which do not, or at most only slowly, react with H_2, form, molecule formation can proliferate. Thus:

$$C + OH \longrightarrow CO + H \quad k = 1.00\,10^{-10}\,cm^3\,s^{-1} \qquad (34)$$

forms CO which is the most abundant molecule in the Universe after H_2 and which takes up essentially all of the available carbon in many environments (recall that in the ISM the elemental abundance of oxygen is greater than that of carbon, table 1). The hydroxyl radical is reactive with a range of atoms and radicals at low temperatures and drives the formation of simple oxides and dioxides:

$$N + OH \longrightarrow NO + H \quad k = 1.00\,10^{-10}(T/300)^{-0.23}e^{-14.9/T}\,cm^3\,s^{-1} \qquad (35)$$

$$S + OH \longrightarrow SO + H \quad k = 6.60\,10^{-11}\,cm^3\,s^{-1} \qquad (36)$$

$$SO + OH \longrightarrow SO_2 + H \quad k = 8.60\,10^{-11}\,cm^3\,s^{-1} \qquad (37)$$

$$CO + OH \longrightarrow CO_2 + H \quad k = 2.81\,10^{-13}e^{-176/T}\,cm^3\,s^{-1} \qquad (38)$$

$$O + OH \longrightarrow O_2 + H \quad k = 3.69\,10^{-11}(T/300)^{-0.27}e^{-12.9/T}\,cm^3\,s^{-1}. \qquad (39)$$

He^+ because of its large ionization potential, generally fragments neutral molecules upon collision, thus generating a population of important reactive ions and radicals, e.g.:

$$He^+ + CO \longrightarrow C^+ + O \quad k = 1.60\,10^{-9}\,cm^3\,s^{-1} \qquad (40)$$

$$He^+ + CH_4 \longrightarrow \text{products including } CH^+, CH_2^+, CH_3^+ \text{ and } CH_3. \qquad (41)$$

2.2. The origin of complexity

The growth of hydrocarbon molecules can occur one C atom at a time through reactions of C and C^+, for example:

$$C^+ + CH_4 \longrightarrow C_2H_3^+ + H \quad k = 1.00\,10^{-9}\,cm^3\,s^{-1} \qquad (42)$$

$$C^+ + CH_4 \longrightarrow C_2H_2^+ + H_2 \quad k = 3.89\,10^{-10}\,cm^3\,s^{-1} \qquad (43)$$

$$C + C_2H_2^+ \longrightarrow C_3H^+ + H \quad k = 1.10\,10^{-9}\,cm^3\,s^{-1}. \qquad (44)$$

$C_2H_3^+$ does not react with H_2 while $C_2H_2^+$ undergoes a slow radiative association:

$$C_2H_2^+ + H_2 \longrightarrow C_2H_4^+ + h\nu \quad k = 1.03\,10^{-14}(T/300)^{-2.01}e^{-7.2/T}\,cm^3\,s^{-1} \qquad (45)$$

so that the C_2-bearing cations recombine with electrons to form C_2, C_2H and C_2H_2. This also enables hydrocarbons to grow in units of C_2, for example:

$$C_2H_2^+ + C_2H_2 \longrightarrow C_4H_2^+ + H_2 \quad k = 4.90\,10^{-10}\,cm^3\,s^{-1} \qquad (46)$$

$$C_2H_2^+ + C_2H_2 \longrightarrow C_4H_3^+ + H \quad k = 9.10\,10^{-10}\,cm^3\,s^{-1} \qquad (47)$$

$$C_4H_2^+ + C_2H_2 \longrightarrow C_6H_4^+ + h\nu \quad k = 1.00\,10^{-9}\,cm^3\,s^{-1} \qquad (48)$$

$$C_4H_3^+ + C_2H_2 \longrightarrow C_6H_5^+ + h\nu \quad k = 2.00\,10^{-10}\,cm^3\,s^{-1} \qquad (49)$$

where the rate coefficients for the last two reactions are calculated values and are valid only for the 10–50 K temperature range.

In general hydrocarbon ions of the type $C_mH_n^+$ are unreactive with H_2 for $n > 4$ and $m > 2$ so that, following dissociative recombination, linear carbon chains such as C_n and C_nH are predicted, and observed, to be abundant in cold clouds. Reactions of radicals and atoms with hydrocarbons create a variety of heterogeneous species:

$$CN + C_2H_2 \longrightarrow HC_3N + H \quad k = 2.72\,10^{-11}(T/300)^{-0.5}e^{-19/T}\,cm^3\,s^{-1} \qquad (50)$$

$$S + C_2H_2^+ \longrightarrow HC_2S^+ + H \quad k = 1.00\,10^{-9}\,cm^3\,s^{-1} \qquad (51)$$

which via analogous reactions involving larger hydrocarbons, produce the cyanopolyynes $HC_{2n+1}N$ (n = 1–5) and C_nS (n = 2–4). Hydrocarbon chains terminated with O, N and S are also observed in these clouds, again the most important hydrocarbon ions in the synthetic chemistry are quasi-stable with respect to reaction with H_2 since these will, in the main, have the largest abundances.

The quasi-stable ions play a significant role in the fractionation of deuterium (discussed in section 2.3) and in the production of large, complex organic molecules via radiative association (recall that in most molecular regions the densities are too low for collisional stabilisation). In this respect the methyl ion dominates via reactions such as:

$$CH_3^+ + H_2O \longrightarrow CH_3OH_2^+ + h\nu \quad k = 2.00\,10^{-12}\,cm^3\,s^{-1} \qquad (52)$$

$$CH_3^+ + HCN \longrightarrow CH_3NCH^+ + h\nu \quad k = 9.00\,10^{-9}(T/300)^{-0.5}\,cm^3\,s^{-1} \qquad (53)$$

$$CH_3^+ + CO \longrightarrow CH_3CO^+ + h\nu \quad k = 1.20\,10^{-13}(T/300)^{-1.3}\,cm^3\,s^{-1} \qquad (54)$$

where the rate coefficients are valid over the temperature range 10–300 K. The ions, following dissociative recombination, lead to the observed interstellar molecules methanol, CH_3OH, methyl cyanide, CH_3CN, and ketene, CH_2CO. In some cases, however, most importantly methanol, the branching channel to the desired neutral molecule, is too small to explain its abundance. The important conclusion, nevertheless, is that radiative association is an important process in the efficient synthesis of large organic molecules in space. Indeed, it is difficult to find any efficient gas-phase mechanism that can form CH_3OH at its observed abundance in interstellar clouds.

Although the above discussion has concentrated on the synthetic power of ion-neutral reactions, those between neutral species can also be important, although only where they are exoergic and do not possess activation energy barriers, for example, the reactions:

$$C_2H + C_2H_2 \longrightarrow C_4H_2 + H \quad k = 9.39\,10^{-11}(T/300)^{-0.2}\,cm^3\,s^{-1} \qquad (55)$$

$$C_2H + C_4H_2 \longrightarrow C_6H_2 + H \quad k = 1.06\,10^{-10}(T/300)^{-0.25}\,cm^3\,s^{-1}. \qquad (56)$$

Figure 6 shows the chemical evolution of selected species as a function of time for a cold (10 K), dark cloud model

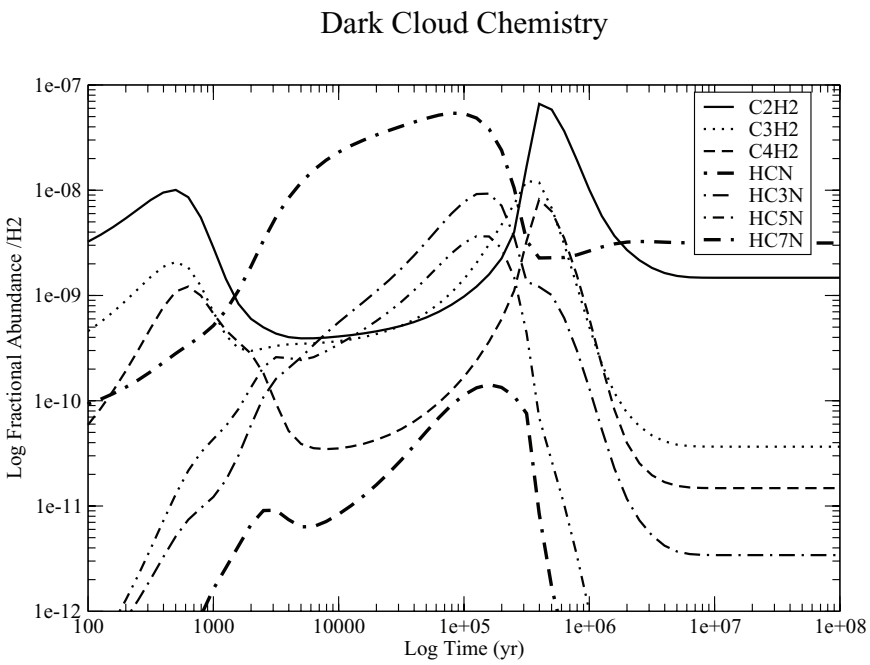

Figure 6. The time-dependent evolution of some hydrcarbons and cyanopolyynes in a cold, dark cloud environment.

at a density $n(H_2) = 10^4$ cm^{-3} when the freeze out of molecules on to the grain surface is ignored. We note that, for molecules possessing a permanent electric dipole moment, rotational transitions are readily observable with radio and sub-millimetre telescopes above fractional abundances of about 10^{-11}–10^{-12}. One sees a number of general trends in this plot. The first is that, at this density, hydrocarbons form fairly rapidly, on a time scale of about 1000 yr due to a rapid conversion of C^+, the initial form of carbon, driven by reaction (7). As the chemistry evolves in this environment, the gas neutralises due to dissociative recombination with electrons and the C^+ is converted into C atoms, which also drive hydrocarbon formation through reaction (31). The abundance of C_4H_2 is closely related to that of C_2H_2 through reactions (46) and (47) and through the neutral-neutral reactions (55) and (56) and its time evolution mimics that of C_2H_2.

The cyanopolyynes form via ion-neutral and neutral-reactions, although the latter tend to dominate. Reactions between CN and polyacetylenes, similar to reaction (50), are particularly efficient; their importance in interstellar clouds has been confirmed by measurements of the various ^{13}C isotopologues in HC_3N and HC_5N which show that, unlike its other carbon atoms, the carbon atom bonded to nitrogen in the cyanopolyynes has the same isotopic ratio as that in CN. The cyanopolyynes do not show the initial abundance peak of the hydrocarbons at 1000 yr due to the difficulty in forming N-H bonds as discussed above. In this case, one sees that their abundances track those of HCN, with peak abundances reached on time scales of a few times 10^5 yr. On longer time scales, essentially all carbon is processed into (unreactive) CO and the abundances of atoms, radicals and molecules fall to steady-state values that are much less than their peak values.

While the above discussion is useful in identifying the main linkages between species and the relevant chemical time scales, it ignores one important process in cold clouds, namely the fact that all species heavier than hydrogen and helium are expected to freeze out onto the surfaces of the dust grains, as discussed in section 1.3.2. Figure 7 shows the effects of accretion onto grains. In this case, the abundance of HCN, for example, is reduced at times less than 10^5 yr and all molecules are removed from the gas around one million years. One consequence of this is that, under the assumption of normal grain properties, cold molecular clouds at high density should be devoid of molecules if they are older than one million years, unless there are non-thermal mechanisms, such as interactions with UV photons or cosmic rays, at work to return ice mantles to the gas.

The most complex interaction of physics and chemistry occurs in protoplanetary disks (section 1.1.3) and is currently a topic of intense research, both observationally and theoretically. Henning and Semenov (2013) give a thorough review of the observations and the range of chemical kinetic models currently in use by the community. In disk systems, photons are generated by three distinct processes: ultraviolet radiation from the central protostar, which includes an excess of Lyman-α emission, and which can be time-dependent in nature due to stellar flares; free-free, or *bremsstrahlung* radiation; and the external interstellar radiation field which can be enhanced above its average value if the PPD sits within an area of active star formation, as happens, for example, in the Orion Nebula. In addition to UV photons, young protostars also emit copious amounts of x-ray photons which have a greater penetrating power than UV and can ionize material deep in the disk. The decay of radionuclides in the disk provides a lower limit to the degree of ionization in the midplane while external cosmic rays can also ionize material deep into the disk, provided they are not shielded by magnetic fields. Figure 8 shows the typical abundance distributions of several molecules, calculated under two approximations, one—labelled 'old'—in which the wavelength-dependence of the photo-cross-sections are

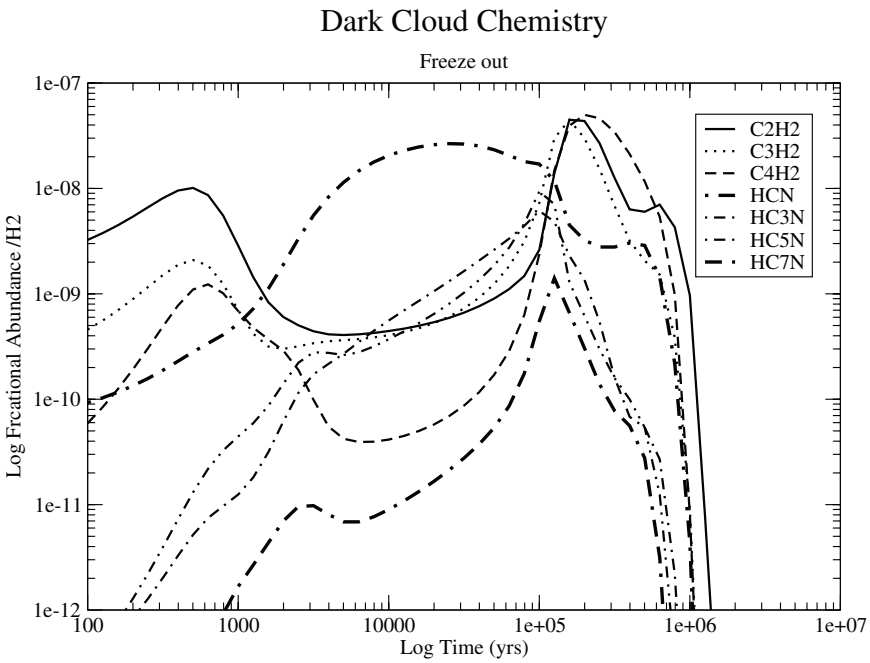

Figure 7. The time-dependent evolution of some hydrocarbons and cyanopolyynes in a cold, dark cloud environment when species are allowed to freeze onto grain surfaces.

ignored. Here, photo-rates are calculated at each of the 12 000 grid points by scaling the interstellar photo-rates by the dust extinction at each point, the other—labelled 'new'—in which the photo-rates are calculated at each point by integrating the wavelength-dependent product of the cross-section and the UV flux.

One sees from these plots that, in general terms, the disk separates into three major chemical regions. The first is the disk surface where the intense radiation fields and high temperatures cause photodissociation and photoionization of the gas. The surface is therefore rich in atomic ions and devoid of molecules. The second region is the midplane layer of the disk in which gas-phase abundances vary dramatically depending on radial distance from the central protostar. Far from the star, typically at distances greater than 10 AU, the combination of high density and low temperatures results in freeze-out of neutral species on to the ice mantles of dust grains. As material flows in towards the central star, the dust grains warm up to a radius where, depending on the particular binding energy of the neutral species in the ice, molecules are thermally desorbed to the gas. Thus, water, with binding energy of around 4800 K, does not evaporate until a radius of just over 1 AU ($\sim$1.5 10^{13} cm), and has a very large gas-phase abundance inside this radius, whereas CO_2, with a binding energy of 2990 K, desorbs at a radius of about 15 AU. It has a large abundance in the midplane between 1 and 10 AU but is destroyed by photons and chemical reactions at smaller radii. The third region evident in these plots is the 'hot molecular layer', seen most clearly in the distributions of H_2O, CO_2 and N_2H^+. This region has a lower boundary where molecules are in solid rather than gaseous form and an upper boundary where they are destroyed by a combination of photons and high-temperature chemistry.

The distributions, however, are also dependent on on poorly-understood physical and chemical parameters, as is evident from figure 8 when one compares the two different approaches to calculation of the photo-rates. While in principle, there is a 'correct' way in which to calculate these, the lack of detailed cross-sections makes this impossible in practice so that approximations need to be made; such approximations can lead to very different distributions. It should also be noted that the intensity and spectral dependence of the UV flux is a complex function of the protostar's mass and age and may be subject to outbursts in intensity due to episodic rather than steady mass accretion. Fogel *et al* (2011), for example, looked at the particular influence of Lyα radiation which in some T Tauri stars can account for 75% of the UV flux. Its influence on molecular distributions depends both on how it is scattered to deep layers in the disk and to the particular values of molecular photodissociation cross-sections at 121.6 nm.

Another area of uncertainty in the chemical modelling of PPDs is the rate at which molecular hydrogen forms on dust grains at low temperatures. The overall formation rate must depend on a number of factors, including sticking coefficients, the nature of adsorption sites and their binding energies, scanning rates of H atoms across the surface, and global grain parameters including size, shape, composition, porosity, etc.

Figure 9 shows the effects of two different approaches for calculating the formation rate of H_2 in molecular clouds. Model A is the 'traditional'—and fairly simplistic—model of Hollenbach and Salpeter (1971) whereas Model B follows the approach taken by Cazaux and Tielens (2002) which considers a range of grain types and properties. This figure, which plots the emergent LTE (local thermodynamic equilibrium) line and continuum spectrum for a face-on disk, shows that emission is very sensitive to the particular choice of the H_2 formation rate, indeed much more sensitive than would appear from consideration, for example, of the vertical column densities in the disk. Model A, in particular, shows weak absorption features in H_2

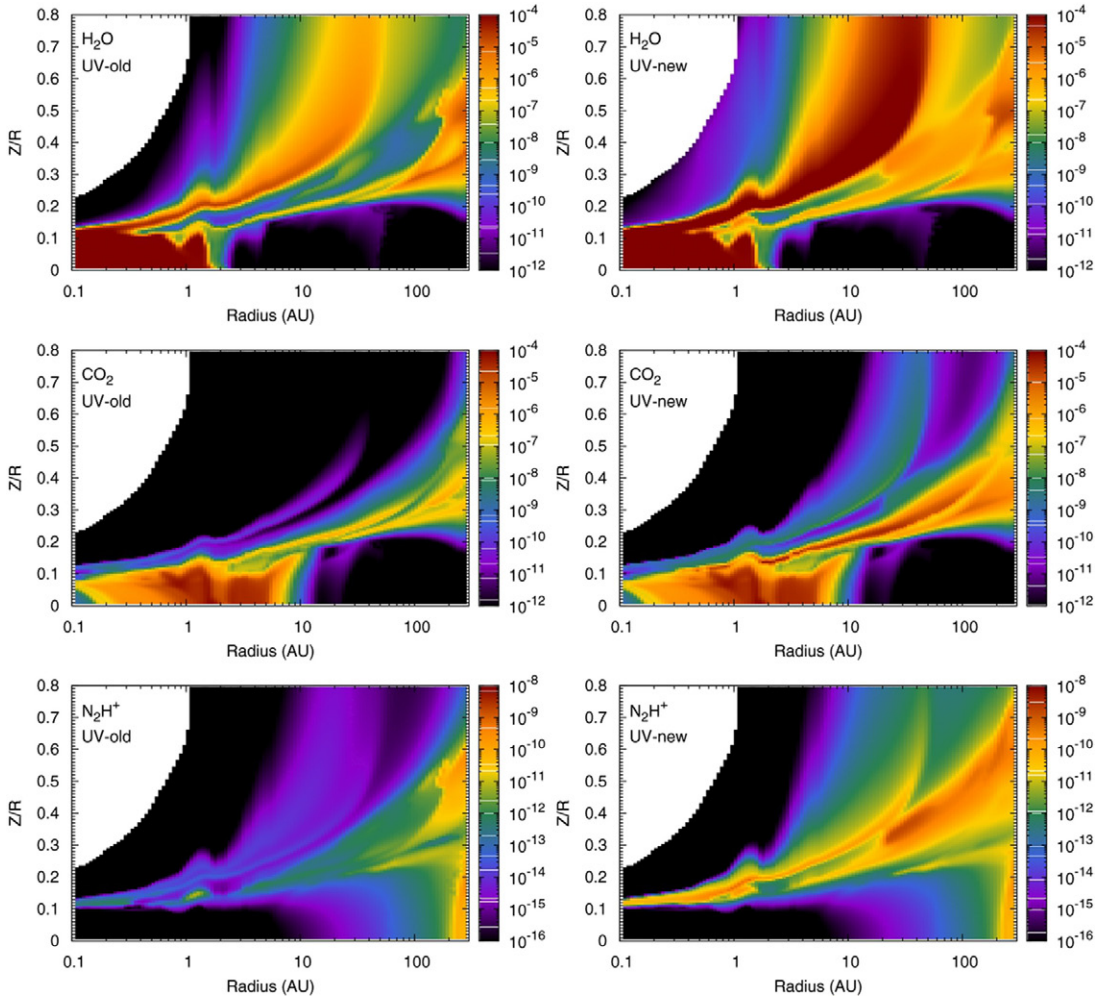

Figure 8. The spatial distribution of some simple molecular species are shown for the typical physical conditions in a disk surrounding a low mass, T Tauri star. These abundances were calculated using the physical model of the disk described in section 1.1.3 (from Walsh *et al* (2012) © 2012. The American Astronomical Society.).

O and CO_2 longward of 10 μm but strong and broad emission lines of H_2O shortward of this wavelength. Absorption lines are due to the fact that both species are abundant near the disk midplane but less abundant in warmer gas closer to the disk surface. The different treatment of H_2 formation in Model B allows for local differences in the H/H_2 ratio to propagate effectively via chemical reactions to other species, in particular to more effective formation of H_2O and OH in warm gas in the disk between 3 and 20 AU. The lines predicted by Model B are stronger than those observed, although this may not necessarily imply that Model B is inappropriate given the fact that the LTE approximation has been used. Non-LTE approaches to radiative transfer generally show that LTE over-estimates the emission by factors of a few.

One important issue often overlooked in studies of the chemistry of PPDs is that of dynamics. Disks are, by definition, dynamical objects. In addition to rotation, material undergoes radial advection and there is evidence, both from our Solar System and elsewhere, that turbulent motions occur in both the radial and vertical directions. In the early stages of star formation, the forming protostar tends to drive bipolar jets perpendicular to the disks which can both affect chemistry, for example through the shock disruption of dust grains, and alter the radiative transfer of stellar radiation by creating cavities in the surrounding gas. The transfer of stellar radiation is also affected by the growth and settling of dust grains and by the creation of holes and rings in the disk through the interaction of newly formed planets with the gas. The global structure and hence chemistry can also be affected by events such as episodic accretion, that is where the accretion rate of matter on to the star is not steady, by stellar outbursts, in which the radiation and particle fields can be enhanced by many orders of magnitude for short periods of time, and by the photo-evaporation of the disk gas by large UV fluxes from the central or nearby stars, a so-called disk wind.

The incorporation of such dynamics into chemical kinetic models is difficult since the dynamical time scales can be comparable to, or shorter than, the chemical time scales. This leads to increased numerical instabilities and results in models which use a much reduced spatial grid. For example, Heinzeller *et al* (2011) have investigated the effects of radial advection, vertical turbulence and disk winds on the abundance distributions in a T Tauri disk. They made a simplifying assumption, given that molecular abundances determine the

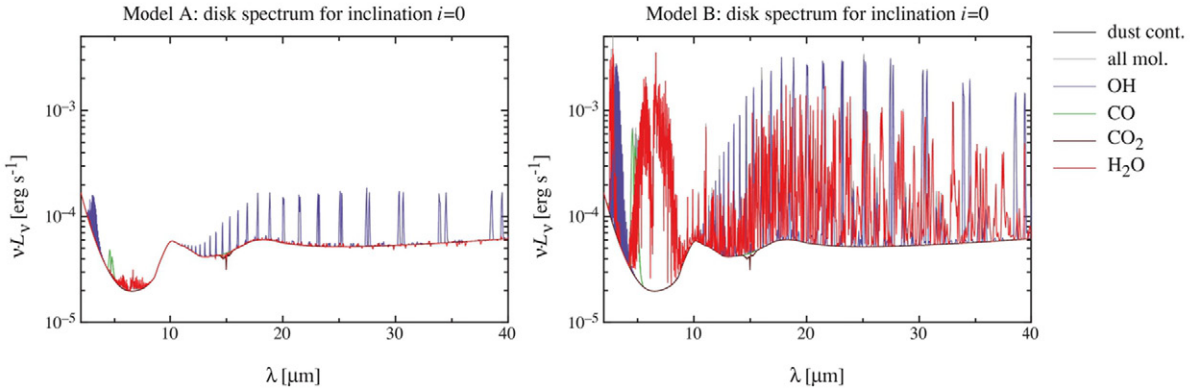

Figure 9. The infrared spectra of a variety of molecules are shown, together with the thermal emission of dust grains, for a face-on disk. Models A and B represent two different approaches to the formation of H_2 on dust grains and can lead to widely different absorption and emission spectra (from Heinzeller *et al* (2011) © 2011. The American Astronomical Society.).

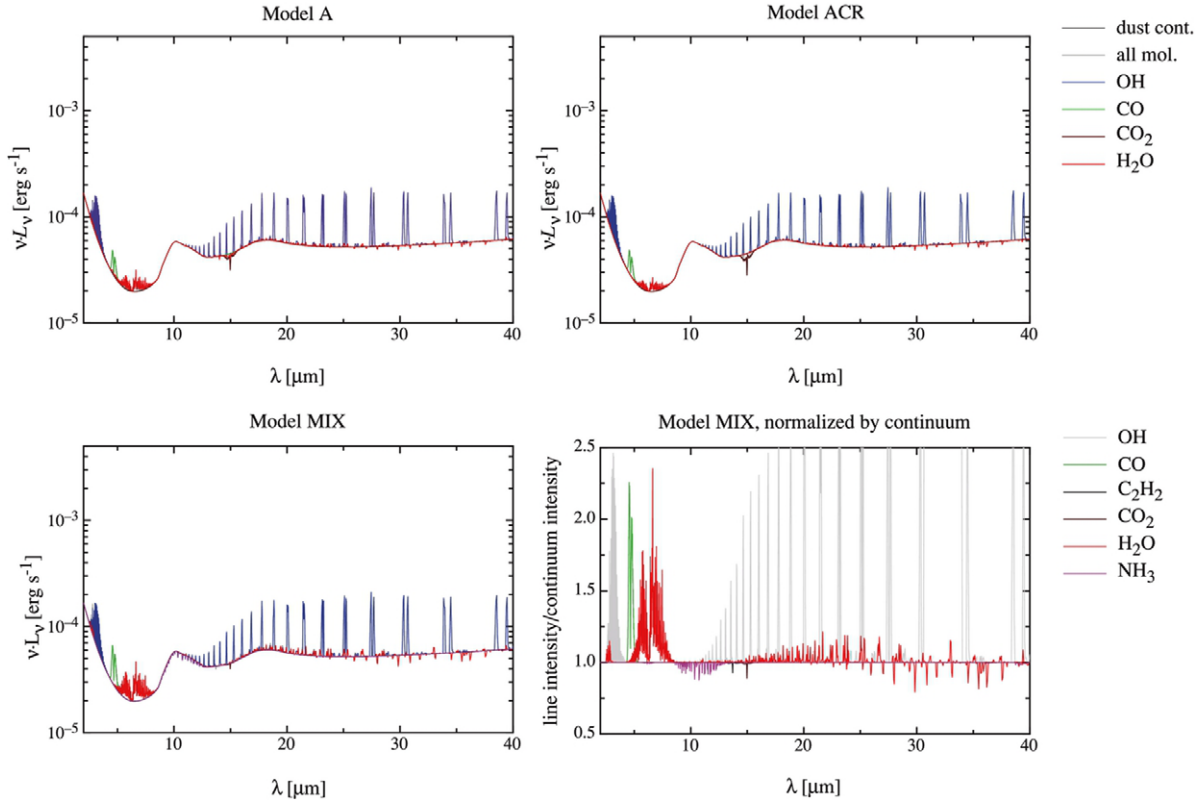

Figure 10. The infrared spectra of a variety of molecules are shown, together with the thermal emission of dust grains, for a face-on disk. Models A is for the steady-state disk, ACR includes the effects of radial advection and MIX incorporates vertical turbulence (from Heinzeller *et al* (2011) © 2011. The American Astronomical Society.).

thermal balance in the disk, that while dynamics influenced the chemical distributions, the new distributions did not feed back into a new physical structure for the disk. They were then limited to a grid of around 400 cells compared to over 12 000 used in the chemical model of a steady-state disk (Walsh *et al* 2012). Figure 10 shows the emergent infrared spectra for three of their models: Model A, discussed above; ACR, in which radial advection is included; and MIX, in which vertical turbulence is included. Furuya *et al* (2013) extended this model to investigate deuterium chemistry in turbulent disks although, as in Heinzeller *et al* (2011), on a relatively coarse grid, around 2000 points in total.

Several authors have considered models which combine chemistry and radiation (magneto)hydrodynamics in a post-processing manner, that is where physical conditions are derived in a flow as a function of time and then chemical kinetic models are evolved using these conditions. Visser *et al* (2011) considered trajectories of material falling on to a PPD in a 2D, semi-analytic approach. More recently, Drozdovskaya *et al* (2014) extended this approach to calculate the chemistry along several hundred streamlines as material flowed on to and in to a disk from a molecular cloud envelope. While this particular paper considered the PPD as the end point of the calculation, other authors have used much more detailed 3D

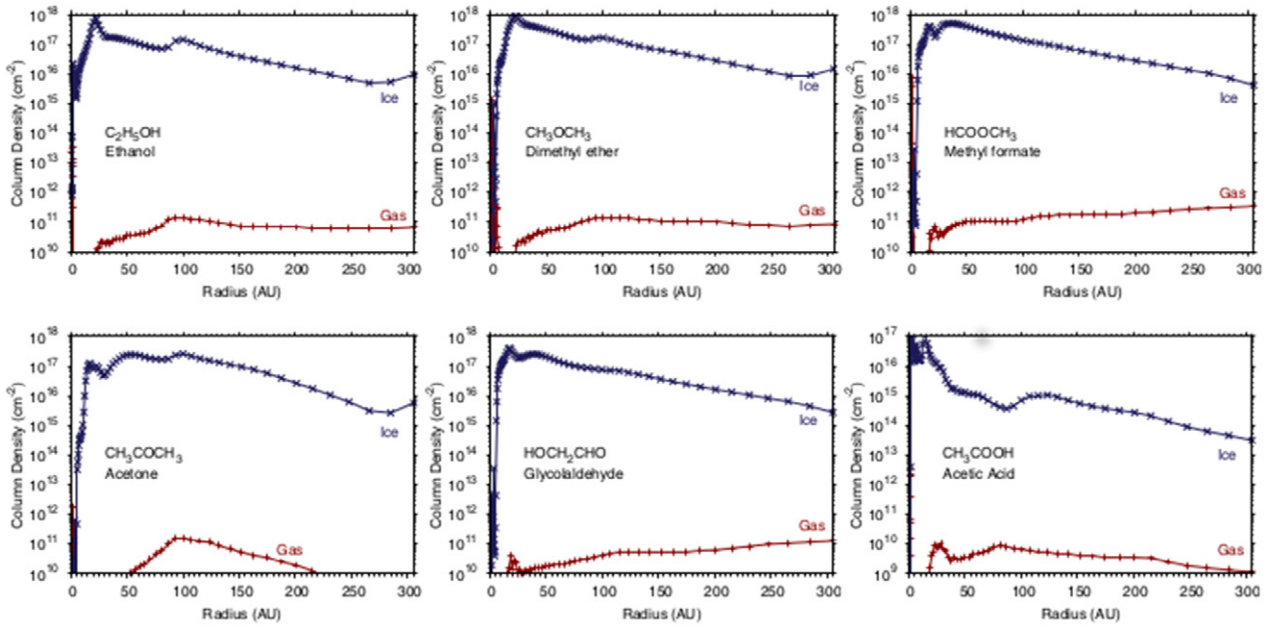

Figure 11. Column densities (cm^{-2}) as a function of radius for gas-phase (red lines) and solid-state (blue lines) species (from Walsh *et al* (2014) © ESO).

radiation magnetohydrodynamic codes to derive physical conditions. One of the most impressive of these models is that by Hincelin *et al* (2013) who followed the collapse of a rotating cloud with an embedded magnetic field up to the point where the first hydrostatic core formed. Even with the simplification of calculating the chemistry once the physical parameters had been determined, they required some 10^4 h of computing time to calculate chemistry along the trajectories of some 10^6 particles. The chemical properties of these first cores are important since it is thought that it is this material which goes on to form the PPD. Finally, we mention the work of Ilee *et al* (2011) who considered the chemistry in a relatively massive, rotating PPD. Such disks, which form around stars with masses greater than the Sun, are subject to gravitational instabilities. These lead to the formation of spiral arms and shock waves which cause molecular abundances to vary on very short temporal and spatial scales. Again, the complexity of the physics allows the chemistry to be followed only for short times, less than 1000 yr in this case.

An interesting question that arises in the study of our Solar System is whether primitive bodies such as comets and meteorites might contain prebiotic molecules thereby enhancing the possibility that the development of life on Earth was enhanced by exogenous delivery. If so, then it is of interest to see whether complex organic molecules, or COMs, can form in abundance in PPDs and perhaps deliver prebiotic material to those exoplanets forming in the habitable zone of protostars.

Walsh *et al* (2014) have investigated this through incorporating a large gas-phase chemistry with an extensive set of surface reactions from Laas *et al* (2011) into their standard disk model with the chemistry of COMs such as propyne, acetaldehyde, methylamine, methyl formate, acetic acid, ethanol, dimethyl ether and acetone included. Figure 11 presents vertical column densities of several COMs as a function of disk radius and shows that COMs are much more abundant in ices than in the gas phase, reflecting the fact that material near the cold and dense midplane dominates the column density. Although it is not entirely clear from this figure, the ice column densities fall off sharply inside a few AU as ice mantles get evaporated with a corresponding rise in the gas-phase column densities. The latter are, however, not as large as the former due to the destruction of gas-phase COMs in the inner disk through a combination of photoreactions and high-temperature chemistry. Walsh *et al* used their calculations to determine disk-integrated line spectra in order to determine the observability of COMs with the new ALMA interferometer but found that their detection in even the nearest PPDs will be challenging, even when the full ALMA configuration becomes available.

COMs can, of course, be detected in interstellar clouds, most notably hot molecular cores, where the evidence is persuasive that there is a significant, if not dominant, contribution to their formation from chemistry occurring in the grain ices (section 1.1.4). The evidence includes the high degree of hydrogenation seen in these molecules, difficult to achieve through H-atom abstraction reactions involving H_2, their relatively high levels of deuterium fractionation, which indicates formation at low temperatures rather than in the high temperature gas in which they are detected, and very high fractional abundances, often many orders of magnitude above those seen in cold clouds.

There have been a number of 'global' mechanisms proposed for such grain ice chemistry. These involve surface hydrogenation of simple, abundant gas-phase atoms and molecules following freeze-out on to the grains, and the interaction between the radicals that are intermediate species. Thus HCO, an intermediate in the hydrogenation of CO to form CH_3OH (Watanabe *et al* 2004), is proposed to dimerise

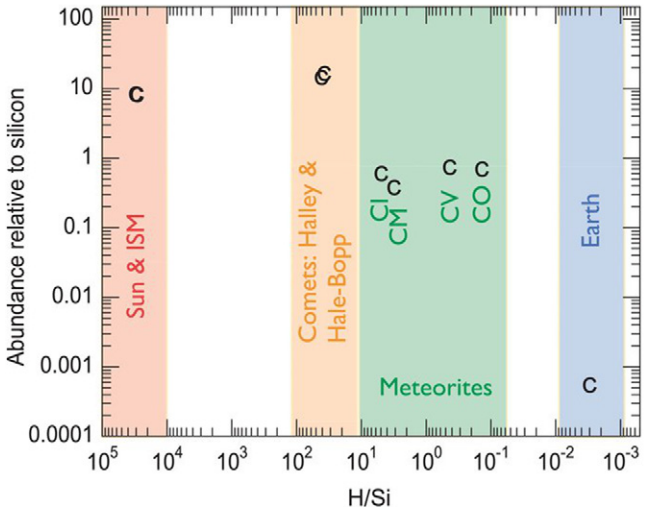

Figure 12. Carbon abundances, indicated by 'C', in the Solar System relative to silicon, showing that carbon is highly depleted in the Earth. Ratios are plotted for four different types of chondritic meteorite (from Lee *et al* (2010) © 2010. The American Astronomical Society.).

followed by H-atom addition to form glycolaldehyde, CH_2 OHCHO (Woods *et al* 2013). Woods *et al* have studied the dimerisation process via DFT calculations and found it to be barrierless and thus a potential source of glycolaldehyde. Dimerisation implies that the HCO radicals are sufficiently mobile to find one another on the surface and will, of course, compete with other reactions, including H addition to form H_2 CO and CH_3OH as well as reaction with other mobile atoms and radicals. Garrod and Herbst (2006) have proposed that in warmer regions such as HMCs, the elevated temperatures, around 20–30 K, of the ice makes radicals sufficiently mobile, either thermally or via quantum tunnelling, that COMs form readily. While such processes may encourage the formation of COMs in warm or hot gas, the recent detection of COMs in cold sources, such as the low mass binary protostar IRAS 16 293–2422 (Jørgensen *et al* 2012), is more difficult to explain in this scenario. A further interesting aspect of this problem is that gylcolaldehyde has two other isomers detected in the interstellar medium, methy formate, $HCOOCH_3$, and acetic acid, CH_3COOH. Gas-phase and grain surface formation mechanisms have been suggested for all but it is as yet unclear which dominate, somthing that will require careful observational and experimental studies. Herbst and van Dishoeck (2009) have summarised the observations of and proposed synthetic pathways to COMs in a relatively recent review.

As well as influencing local molecular abundances and therefore emission, the interaction between the gas and grain species can also have global impact. An important example, very relevant to the Solar System, is the sequestration of carbon in CO which can influence to a significant degree the amount of carbon available for organic molecules. Figure 12, taken from Lee *et al* (2010), shows the variation in the carbon/silicon ratio compared to the hydrogen/silicon ratio in a number of astronomical environments and shows that the amount of carbon in the Earth's mantle is highly depleted compared to the amount of carbon available at the formation of the Solar System, the Solar/ISM value. This appears to be true even if one takes into account that one is not able to measure the amount of carbon in the Earth's core. Indeed one sees that carbon depletion is also apparent in meteoritic bodies indicating that, more generally, it is difficult to incorporate carbon into refractory bodies despite the fact that the carbon abundance appears normal in the cooler materials that reside in the outer Solar System.

Lee *et al* (2010) suggest that carbon grains, transported into the inner Solar System, are eroded by thermally hot oxygen atoms in a region above the midplane, a region in which oxygen atoms are produced by photodissociation and grains are suspended by turbulent stirring. This chemical erosion occurs for carbon grains but not for silicate grains which survive to form the terrestrial planets. Since this process results in gas-phase carbon that either accretes on to the star or is lost to the system, the carbon found on Earth must be delivered, with water, in the form of carbon-bearing ices by cometary impacts.

An alternative explanation has been suggested by Favre *et al* (2013) who used Submillimetre Array (SMA) observations of CO and Herschel Space Observatory measurements of HD toward the TW Hya disk to show that gas-phase CO was depleted by a factor of around 10 compared to the expected C/H ratio in the warm molecular layer that is probed by the observations. Favre *et al* infer that CO is destroyed through reaction with He^+ with the C^+ produced being processed into hydrocarbon molecules while the O atoms form H_2O. These molecules, which have larger binding energies to water ice than CO, freeze out on to grain surfaces and can be transported more efficiently to the inner PPD than the volatile CO molecule.

2.3. Deuterium fractionation

One of the surprising results of early radio astronomical observations of interstellar molecules was that D/H ratios in molecules such as HCO^+ and HCN were enhanced significantly, or fractionated, over the cosmic D/H ratio, $(D/H)_C \sim 2 \times 10^{-5}$, set by nucleosynthesis in the Big Bang and the limited amount of astration, i.e. the destruction of deuterium in stars, that has occurred since then. Table 4 lists those species detected to date in interstellar clouds.

It was quickly realised that quasi-stable molecular ions were key to understanding fractionation. Three major processes are initiated by D-fractionating reactions involving the 'bath' of deuterium in dense clouds, HD:

$$H_3^+ + HD \leftrightarrow H_2D^+ + H_2 \qquad \Delta E_1/k = 232\,\mathrm{K} \tag{57}$$

$$CH_3^+ + HD \leftrightarrow CH_2D^+ + H_2 \qquad \Delta E_2/k = 352\,\mathrm{K} \tag{58}$$

$$C_2H_2^+ + HD \leftrightarrow C_2HD^+ + H_2 \qquad \Delta E_3/k = 550\,\mathrm{K}. \tag{59}$$

These reactions are exoergic in the forward direction by energies which are given for ground state reactants. Thus, at the low temperatures of cold dark clouds, the back reactions do not proceed and the H_2D^+/H_3^+ abundance ratio can be much larger than that of HD/H_2. To get an estimate of the

Table 4. Deuterated molecules detected in interstellar clouds.

Number of atoms							
2	3	4	5	6	7	8	9
HD	DCO^+	HDCO	c-C_3HD	CH_2DOH	CH_3CCD	$HCOOCH_2D$	CH_2DOCH_3
ND	DCN	D_2CO	c-C_3D_2	CH_3OD	CH_2DCCH	$DCOOCH_3$(?)	
OD	DNC	HDCS	NH_3D^+	CHD_2OH	DC_5N		
	HDO	D_2CS	DC_3N	CD_3OH			
	HDS	NH_2D	C_4D	CH_2DCN			
	D_2S	NHD_2	CH_3D(?)	HDCCCC			
	H_2D^+	ND_3					
	HD_2^+	l-C_3D					
	N_2D^+						
	C_2D						
	D_2O						

enhancements possible, consider H_2D^+ which has additional loss reactions through dissociative recombination with electrons and reaction with neutral species, M. Then, assuming steady state for simplicity

$$R(H_2D^+) = \frac{f(H_2D^+)}{f(H_3^+)} = \frac{k_f f(HD)}{k_r + k_e\, f(e) + \Sigma k_M f(M)} = S_{H_2D^+} R(HD) \quad (60)$$

where k_f and k_r are the forward and reverse rate coefficients of (57), $f(X)$ represents the fractional abundance, $n(X)/n(H_2)$, of species X, M = CO, O, N_2, H_2O, etc and $S_{H_2D^+}(T)$ is the enhancement factor which is a function of T. For conditions typical of cold, dark clouds the third term in the denominator dominates and $S_{H_{2D}^+} \sim 1/\Sigma f(M) \sim 10^3 - 10^4$, that is, $R(H_2D^+)$ ~0.01–0.1. For $T \sim 20$ K, the back reaction with H_2 becomes important and $R(H_2D^+)$ decreases exponentially with increasing temperature—thus, this fractionation process is unimportant at room temperature.

Radiative association of H_2 with CH_2D^+ and C_2HD^+ competes with the back reactions in (58) and (59) so that the behaviours of $R(CH_2D^+)$ and $R(C_2HD^+)$ differ in detail from that of $R(H_2D^+)$. The general conclusion, however, is that each of the quasi-stable ions can be significantly fractionated in deuterium below a critical temperature that is approximately one-tenth of the value of the appropriate endothermicity.

This initial fractionation in the ions can be passed on to other species through subsequent reactions. Thus, in collision with CO, H_2D^+ can transfer either a deuteron or a proton, with statistically one-third of reactions producing DCO^+ rather than HCO^+:

$$H_2D^+ + CO \longrightarrow DCO^+ + H_2 \quad (1/3) \quad (61)$$

$$H_2D^+ + CO \longrightarrow HCO^+ + HD \quad (2/3). \quad (62)$$

Since the loss mechanisms of DCO^+ and HCO^+ are essentially the same, this leads to the prediction that $R(DCO^+) \sim R(H_2D^+)/3$ and similarly for other protonated ions such as N_2D^+ and DCS^+. The observational determination of the DCO^+/HCO^+ ratio in cold clouds thus leads to an estimate of the fractional ionization, $f(e)$, an important parameter in controlling the star formation process. This can be achieved by using (60) since the rate coefficients and the CO abundance, the major contributor to species M, can be measured. In addition, and importantly, the dissociative recombination of H_2D^+ leads to an enhanced atomic D/H ratio. This enhancement can lead directly to a large fractionation in, for example, gas-phase OD:

$$D + OH \longrightarrow OD + H \quad (63)$$

which is exothermic by about 800 K (Croswell and Dalgarno 1985). Croswell and Dalgarno predicted OD/OH ratios of a few percent in dark clouds. The large gas-phase atomic D/H ratio also leads, through collisions with grains, to an enhanced D/H ratio on ice mantles which can drive a D-rich chemistry on the surface. It is this chemistry that is believed to be the source of high D/H ratios measured in gas-phase molecules in hot molecular cores as discussed in section 1.1.4.

In very cold dense regions, all molecules, with the exception of hydrogen and its ions, will collide with and freeze-out on to dust grains on a rapid time-scale (section 1.3.2). This leads to the situation where the molecules that are routinely observed in order to derive physical conditions in dark clouds, for example, CO, HCO^+, HCN, CS, NH_3 etc, are no longer present in the gas phase. In such regions, however, new species become abundant. In these objects, HD remains in the gas and can further deuterate H_3^+ to D_3^+ in the reaction chain:

$$H_3^+ + HD \longrightarrow H_2D^+ + H_2 \quad (64)$$

$$H_2D^+ + HD \longrightarrow D_2H^+ + H_2 \quad (65)$$

$$D_2H^+ + HD \longrightarrow D_3^+ + H_2 \quad (66)$$

with the only competition being dissociative recombination with electrons. One finds that, under these conditions, D_3^+ can be more abundant than H_3^+ and that atomic D/H ratios in the gas and on the grains can be larger than unity. This has important implications for deuterating the trace amounts of neutral species that remain in the gas as well as driving fractionation via grain surface reactions. Thus, for example, Brown and Millar (1989) showed that the OD/OH ratio could be as large as unity due to the D + OH reaction. Recently this has been

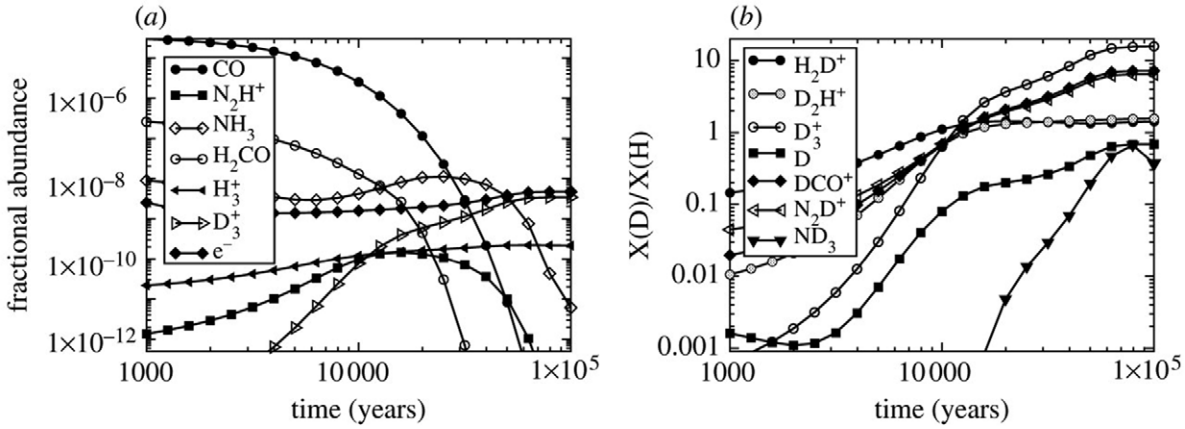

Figure 13. Fractional abundances (a) and D/H ratios (b) calculated for a variety of molecules for a model in which $T = 8$ K and $n(H_2) = 10^6$ cm^{-3} (from Roberts and Millar (2006)).

verified by the detection of OD at 1.392 THz using SOFIA, the Stratospheric Observatory for Infrared Astronomy, in the cold low-mass proto-binary source IRAS 16 293–2422, a source which contains very large abundances of multiply-deuterated molecules including D_2CO and CD_3OH (Parise *et al* 2004, Parise *et al* 2012). Although it was not possible to derive the OD/OH abundance—OH is unobservable with SOFIA and although observable at centimetre wavelengths, these do not allow an accurate ratio to be derived since they sample completely different gas, both spatially and in density. Nevertheless, Parise *et al* infer a very large abundance of OD by comparing it to HDO with OD/HDO ∼17–90. It is precisely in these cold (10 K), dense (10^6–10^8 cm^{-3}), regions that doubly and triply deuterated molecules, such as D_2S, D_2CO, CD_3OH, and ND_3, are observed. Figure 13, from Roberts and Millar (2006), shows the fractional abundances and D/H abundance ratios for a number of species for the particular case of a cold, dense cloud in which accretion onto grains occurs on a time-scale of about 10^4 yrs. It shows that D/H ratios in the hydride ions can reach extremely large values, greater than unity, and can enhance the fractionation in other molecules; the abundance ratio of ND_3/NH_3, for example, is greater than 0.1 at cloud ages beyond 40 000 yrs.

These regions of enhanced accretion on to grains do allow for the presence of newly observable species to probe the physics of the gas, namely H_2D^+ and D_2H^+, both of which possess small permanent electric dipole moments, and have allowed rotational transitions in the sub-millimetre range, unlike H_3^+ and D_3^+. The new generation of sub-millimetre telescopes on high dry sites, such as the single-dish APEX telescope and the ALMA 66-dish interferometer situated at an altitude of 5000 m in the Atacama Desert, (figure 14), will finally enable us to study the end point of the collapse of molecular gas to form stars.

The detailed fractionation driven by D_2H^+ and D_3^+ was first described by Roberts *et al* (2003) but it was Flower *et al* (2004) who noted that the detailed energetics of the reactions leading to D_3^+ would be affected by the rotational states, ortho, para and meta, occupied by the reactants and by nuclear spin conservation rules (Oka 2004, Hugo *et al* 2009). As an example, at 10 K, H_2 can be found either in its $J = 1$ (ortho) or $J = 0$ (para) states with $E(J = 1) - E(J = 0) = 170$ K—radiative transitions between $J = 1$ and $J = 0$ states are not allowed. Thus the back reactions of (57)–(59) possess energy barriers that are significantly reduced for collisions involving $H_2(J = 1)$. This would not be significant in cold (10 K) clouds if H_2 was in local thermodynamic equilibrium but this does not appear likely (the rotational populations of H_2 cannot be determined directly in these regions since H_2 is unobservable). The excess energy, 4.5 eV, associated with H_2 formation on dust grains sets the initial ortho-para ratio in H_2 to 3:1, the high temperature limit. The ortho-para ratio can be altered through proton exchange reactions of H^+ and H_3^+ with H_2 but this is a slow process at the low temperatures and low ionization levels in dark clouds, and takes much longer than 10^7 yr, i.e. significantly greater than the cloud lifetime, $\sim 10^6$ yr, to reach the LTE value of 2×10^{-7} (Pagani *et al* 2009). In dark clouds the ortho-para ratio of H_2 is likely between 0.1 and 0.001, sufficient to decrease the fractionation of H_2D^+ and related ions from the very high values given by the simple approximations above.

Although inclusion of quantum effects lowers the efficiency of fractionation in the gas phase, the fractionation of H_2D^+, D_2H^+ and D_3^+ leads to large atomic D/H ratios and thus to large fractionation in OD via the gas-phase reaction (63) and on grain ice mantles following accretion of D atoms. The influence of nuclear spin on the fractionation of the hydrogen species is shown in figure 15 (Sipilä *et al* 2010) which compares the steady-state abundance ratios as a function of density for two sets of state-to-state rate coefficients (Flower *et al* 2004, Hugo *et al* 2009). These results are equivalent to the long-time evolution in the calculations by Roberts and Millar (2006), that is, in the regime where all elements heavier than H and He are removed from the gas.

These plots confirm the results of Roberts and Millar, namely that very large fractionation ratios can arise in dense, cold gas when heavy elements are frozen out on to grain surfaces. They show that, in addition, the detailed abundances depend on the specific rotational populations and the spin-selection rules applied to the reactions. As shown by Sipilä *et al*, an accurate calculation of the state-to-state chemistry is essential to accurately interpret observations of H_2D^+ and

Figure 14. A night-time view of the 66-element ALMA interferometer. The two irregular galaxies in the picture are the Large and Small Magellanic Clouds. (Photo credit: ESO.org Christoph Malin).

D_2H^+ in dense cores. If the grains play only a passive role in influencing gas-phase molecular abundances, that is simply through acting as a sink for molecules, then it is is clear that these deuterated ions give us a unique probe of the late stages of cloud collapse and the early stages of star formation. The situation is less clear, however, if deuterium takes part in an active surface chemistry. Sipilä *et al* (2013) have argued that D atoms, which will be heavily fractionated relative to H atoms due to recombination of abundant D_3^+ for example, will react on icy surfaces to form HDO and D_2O rather than re-cycle to HD. The net effect is to reduce the abundance of HD in the gas, since the deuterated ions are produced in reactions that involve HD. The outcome can be severe—Sipilä *et al* show that the HD abundance can be reduced by two to three orders of magnitude between 10^6 and 10^7 yrs for gas at a density of $n(H_2) = 10^6$ cm^{-3}. This has very significant implications for the chemistry since all deuterated species will be depleted in the high density cores of clouds—Sipilä *et al* find that fractionation is larger at core edges than at core centres—and that HD can not be used as a proxy for the H_2 abundance and mass, an assumption used by Favre *et al* (2013) in their study of CO depletion in the TW Hya PPD as discussed in section 1.1.3. If HD is, in fact, depleted in the disk region probed by the SMA, then the CO/H_2 ratio in the gas may be normal and the extraction of carbon from CO and its incorporation into hydrocarbons may not be the explanation the carbon abundance anomaly in the Solar System. The detailed surface chemistry of deuterium is thus an important topic for laboratory investigation.

2.4. Isotopic fractionation

Enhancements of heavy isotopes of other elements are observed in interstellar molecules but are generally much less than those of D because of smaller zero-point energy differences. In diffuse clouds, for example, where photoionization ensures that C^+ is the dominant isotope bath, the reaction:

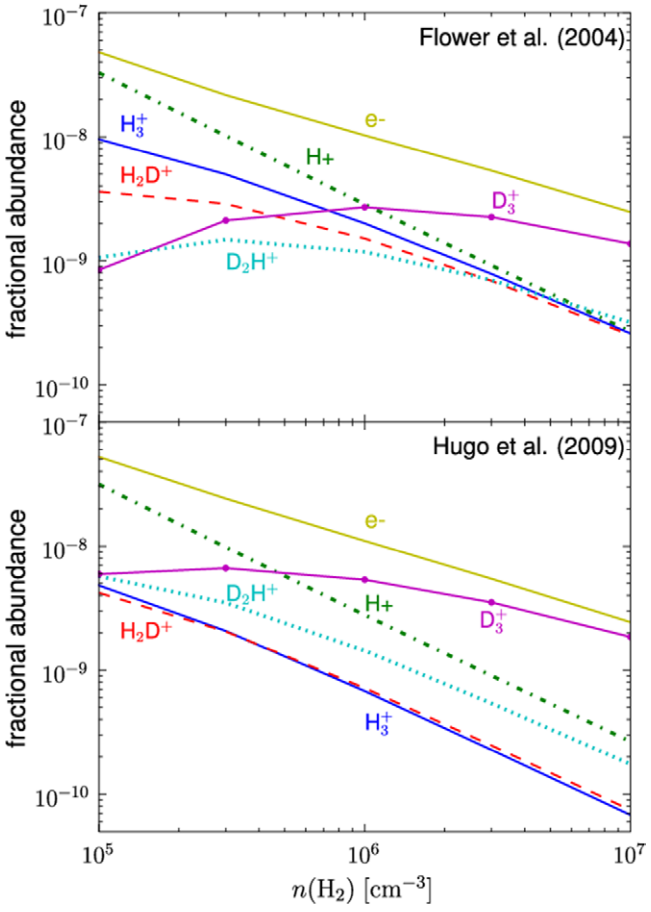

Figure 15. Steady-state fractional abundances calculated at 10K as a function of density for two choices of the state-to-state rate coefficients (from Sipilä *et al* (2010) © ESO).

$$^{13}C^+ + ^{12}CO \longrightarrow ^{12}C^+ + ^{13}CO \qquad (67)$$

with $\Delta E/k \sim 35$ K, enables $^{13}CO/^{12}CO$ to be larger than the $^{13}C/^{12}C$ elemental ratio. The effect is not large however and is

limited in such clouds because photodissociation of CO occurs though the line absorption of UV photons, with the result that ^{12}CO self-shields, i.e. the particular UV photons capable of dissociating ^{12}CO are absorbed, before ^{13}CO, which has a smaller abundance, self-shields. Thus, the photodissociation rate of ^{13}CO is slightly larger than that of ^{12}CO, thereby reducing the ^{13}CO enhancement driven by the C^+ reaction. The overall outcome is that $^{13}CO/^{12}CO$ is slightly enhanced, and that of $^{13}C^+/^{12}C^+$ slightly decreased, below the cosmic (or local) value. As is the case for deuterium, this enhancement/depletion can be passed on to other species depending on the chemical network. Thus HCO^+ will reflect the CO isotopic ratio since it is formed directly by the proton transfer reaction:

$$H_3^+ + CO \longrightarrow HCO^+ + H_2 \qquad (68)$$

whilst other species, for example CN and HCN, formed via reactions involving simple hydrocarbons such as CH and CH_2, reflect the depleted ratio in $^{13}C^+$.

Fractionation can also occur in O, N, and S although the effects are small and difficult to measure unambiguously through molecular line observations.

2.5. Grain surface chemistry

As indicated in section 1.3.2, it is expected that all species, with the exception of H_2, He and their ions, will freeze out on to the surface of cold dust grains on relatively short timescales in dark clouds. For a grain of radius 0.1 μm and around 10^6 binding sites on its surface, the removal of all O, C and N species from the gas will result in the growth of around 200 layers of 'ice'. This ice mantle is most easily observed through infrared absorption spectroscopy which traces vibrational transitions. Since one needs a bright infrared star behind or embedded within a cold, dark cloud to perform the observations, and because the Earth's atmosphere absorbs IR photons, relatively few objects have been well-studied using ground-based telescopes. The advent of orbiting observatories, such as the Infrared Space Observatory, ISO, and in particular the Spitzer Space Telescope, have enabled detailed studies of ice composition in a variety of objects. As mentioned previously, one important limitation is that detections are sensitive only to fractional abundances that are greater than $10^{-7}-10^{-6}$ relative to H_2 or about 0.1–1% of the abundance of water ice.

A typical IR spectrum of a cold dark cloud is shown in figure 4 with the main absorption bands identified. Table 5 presents the derived abundances toward three types of sources, low- and high-mass protostars embedded in molecular clouds and toward background sources, i.e. stars which lie beyond the molecular cloud and which cannot be influencing the composition and characteristics of ice mantles (Öberg *et al* 2011). Water ice is found to be dominant with CO, CO_2 and CH_3OH the next most abundant species. Abundances of these and other more minor species such as H_2CO, HCOOH, CH_4 and NH_3, vary from object to object, perhaps reflecting local conditions and time scales. Table 5 lists the relative abundances of the most common species in ices. Detailed comparison of the interstellar ice band profiles with laboratory experimental data leads to the conclusion that interstellar ices are segregated or layered and that CO, for example, is found in both non-polar (dominated by CO and CO_2) and polar (predominantly H_2O) components.

Table 5. Abundance medians for components of individual ices and individual ice components toward low- and high-mass protostars and through dark clouds toward background stars (from Öberg *et al* (2011)).

Ice	Low mass	High mass	Background
H_2O	100	100	100
CO	38	13	31
CO_2	29	13	38
CH_3OH	7	8	8
NH_3	5	15	—
CH_4	5	4	—
XCN	0.6	0.8	—
Pure CO	21	3	—
CO:H_2O	13	10	—
CO:CO_2	2	1.3	—
Pure CO_2	2	2	—
CO_2:H_2O	20	9	24
CO_2:CO	5	5	6

The most important reactive species on cold grain surfaces is atomic hydrogen due to its low binding energy and its ability to diffuse, either thermally or quantum mechanically, across the grain. To a first approximation, atomic hydrogen can be considered mobile, with heavier species fixed to particular surface sites. This, together with its relatively high abundance, means that, for example, O atoms accreting on to the surface are rapidly hydrogenated to form water, consistent with the high fractional abundance seen in the IR absorption bands—around 100 times more water is contained in ice than in the gas phase.

An accurate description of a detailed grain surface chemistry is made more difficult because of the number of fundamental issues which are very poorly understood at present. These include the detailed physical properties of the underlying grain, its composition, morphology, porosity, distribution of surface sites and their binding energies, surface versus bulk chemistry, and by processes which at first glance may be too slow to be significant, but which may not be so given typical ice mantle lifetimes of $10^5 - 10^6$ yr in cold clouds. These processes include the interaction of cosmic rays and UV radiation with the dust.

Once the nature of the grain and its surface have been defined (at least for modelling purposes), one can begin to describe the chemical processes that occur which are typically one of two mechanisms: (i) Eley–Rideal, in which an incoming gas-phase reactant collides directly with an absorbed reactant, and (ii) Langmuir–Hinshelwood, in which two reactants interact following diffusion, either thermally or quantum mechanically. Mechanism (ii) therefore requires at least one of the reactants to be bound to the surface through physisorption rather than chemisorption. Under normal cold dark cloud conditions, that is, where grains are covered in ices, physisorption and diffusion dominates and therefore reactions involving mobile H and D atoms tend to dominate the chemistry.

A final fundamental issue is that rate equations, routinely used to describe gas-phase chemical kinetics, may not be appropriate when describing surface chemistry on interstellar grains, since the use of average concentrations, central to the rate equation description, has limited use in kinetics when the average number of reactive species becomes less than one per grain. Thus, for example, a grain containing one H atom on its surface cannot form H_2, whereas an approach using the average surface concentration, the rate equation approach, would calculate a non-zero rate coefficient for H_2 formation. In addition, if the diffusion rate of a particle on the surface is large and the gas density small, so that collisions with the grain are rare, the surface particle is likely to react with the first particle that lands on the grain, the so-called 'accretion limit'.

The most accurate way to treat surface chemistry in this limit is to use stochastic methods, that is, through solving the master equation, in which one describes the change in time of the probability density function of this system. Here, one associates a probability density $\Phi(\bar{N}, t)$ with state $\bar{N}$ at time t, where $\bar{N}(t) = [N_1(t), N_2(t), ..., N_k(t)]$ is described by the number of particles, $N_i(t)$, of each species at time t, and which changes with time due to chemical reactions. Thus, for example, chemistry on a surface can be represented by chemistry on a set of lattice points, each corresponding to a surface site, with the population at each point described by the state vector $\bar{N}$.

Because of the stochastic nature of this approach, computational time can be long and several approximations are normally made in interstellar studies:—(i) all sites are identical, so one can follow the total number of each species on the surface, and (ii) the distribution of particles on the surface is random. The terms equivalent to rate coefficients in gas-phase chemistry then depend, for reactive species *i* and *j*, on the times taken for the species to scan the grain surface, on the presence of an activation energy barrier, and on a combinatorial factor.

One sees that a stochastic approach can lead to an 'infinite' number of possible states, if, for example, one associates a probability to every possible state of the system. One can reduce the equations to a finite set by imposing a 'maximum population', a valid approximation given that the stochastic approach is needed only when the number of reactants is small. Solution of the master equation then gives the probabilities for each of these finite number of states from which the expectation values $< N_i >$ of each species can be derived. Such an approach is computationally intensive, particularly when compared to a gas-phase chemistry, and is limited to the treatment of only a few surface species (e.g. Stantcheva and Herbst (2004)).

An alternative to the direct solution of the master equation is to use Monte Carlo methods although a large number of model calculations must be made in order to obtain convergence (Caselli *et al* 1998, Charnley 1998). Cuppen and Herbst (2005) and (2007) have pioneered the use of Continuous Time Random Walk (CTRW) microscopic Monto Carlo methods in astrochemistry. In their work, they follow the path of every particle on every site in a model surface. Their description allowed for site-specific properties, e.g. a variety of binding energies, and for multi-layer growth of ice on the surface, and considered both H_2 formation and the growth of ice mantles. Cuppen and Garrod (2011) used the same technique to investigate H_2 formation on dust grains containing surface irregularities that is, sites possessing different binding energies, and have shown that the modified rate equations can be used to reproduce the CTRW results as long as the population of 'strong' binding sites is less than about 30%.

The major drawback of such microscopic models is their computational expense which limits the time scales and number of species that can be described. Vasyunin and Herbst (2013) have described a macroscopic Monte Carlo model that incorporates both gas phase and grain surface reactions, in total around 6000 reactions describing the chemistry of 660 species. They argue that their results, which are calculated for times up to 10^6 yr, are more exact although computational times are still long. One approach to reducing computational effort was introduced by Lipshtat and Biham (2004) who noted that the chemical system is sparse, that is, most species react with only a few others. If it is assumed that unreactive species are conditionally independent of each other, than the number of equations in the master equation approach can be reduced dramatically. This multiplane method has been shown by Barzel *et al* (2010) to be in good agreement with the direct solution of the master equation. Barzel and Biham (2011) also showed that moment equations generated from the master equation could be used in an efficient manner. The generation of moment equations results in the problem that higher-order moments appear, thus making closure difficult. Barzel and Biham (2011) and Barzel and Biham (2012) showed that the moment equations could be expressed in terms of so-called binomial moments, linear combinations of ordinary moments, which captured the essential physics, but allowed for a much-reduced set of linear equations, rising polynomially with the number of reactive species, rather than the exponential increase which results when using the master equation approach. The moment method generates one equation for each species and one equation for each reaction. While ordinary moment equations are often adequate, Barzel and Biham (2012) show that binomial moments allow for a greater range of chemical processes, have an intuitive physical meaning and lead to easily writable forms of the equations, while giving excellent agreement with the more complete Monte Carlo methods.

While there are a variety of stochastic approaches developed for situations such as cellular chemistry, where the number of reactant molecules can also be small or not well-mixed—see Gillespie *et al* (2013) for a review of these techniques—their use in astrochemical models is still at an exploratory level. The interested reader is referred to a recent review by Cuppen *et al* (2013) on the use of stochastic models in describing surface chemistry on interstellar dust grains.

One of the key motivations behind such studies is to discover whether the fundamental chemistry that drove the emergence of life on Earth was restricted to the planet itself or whether it could have had a contribution from chemical processes that occurred in space, either in molecular clouds or in protoplanetary disks. Interstellar and cometary ices are a potential delivery mechanism so a number of experiments

have been undertaken, involving thermal and non-thermal processes, to answer this question. Indeed gylcine, confirmed as extraterrestrial in origin through its $^{13}C/^{12}C$ ratio, has been detected in the material sampled by the *Stardust* comet return mission to comet 81P/Wild 2 (Elsila *et al* 2009). There are a range of non-thermal processes which are known to drive molecular synthesis. Thus, the interaction of UV and x-ray photons and high-energy particles such as electrons and ions with ices leads to the formation of quite complex species in the ice. Ciaravella *et al* (2012) have irradiated pure CO ices with soft x-rays and find the formation of a range of carbon oxides including CO_2, C_2O, C_3O_2 and C_4O. An interesting set of complex organic molecules is formed if methanol ice is used. Chen *et al* (2013) detect the presence of CH_2OH, CH_4, acetic acid CH_3COOH, methyl formate $HCOOCH_3$, dimethyl ether CH_3OCH_3 and ethylene glycol $(CH_2O)_2$, all observed interstellar molecules, amongst others. Here the chemistry is mediated by the generation of secondary electrons with an energy distribution that is dependent on the energy of the x-ray photons. The interaction of x-rays with ice mantles is likely to be important in PPDs (section 1.1.3) since young stars can be strong emitters of x-rays and the penetration depth into the disk is larger for x-rays than for UV photons, which can also generate complex species when they interact with methanol ice (Öberg *et al* 2009). Ongoing experiments are needed, not only to investigate the formation of complex molecules but also to see if the kinetics of their formation can be understood through either the use of deterministic or stochastic models. If successful, this would provide a degree of comfort in extending models to the interstellar environment where interactions with the grains occur at the single photon/particle level.

2.6. Shock waves in molecular clouds

It has been known for around 40 years that molecular emission lines, particularly those in regions of star formation, have line widths that can be highly supersonic, up to several hundred km s^{-1} in some cases. The presence of such motions, which can often be traced through ro-vibrational emission from H_2, one of the very few instances in which H_2 is visible to our telescopes, is likely due to the propagation of pressure disturbances or shock waves through interstellar gas. These can be generated by a multiplicity of processes, including stellar jets and winds, cloud-cloud collisions, and stellar explosions, such as novae and supernovae. Since shocks compress and heat the gas, they can induce chemical reactions that would not otherwise occur and cause both excitation and abundance conditions such that we can probe the shock physics in some detail. Shocks can also disrupt, and indeed destroy, interstellar grains through both sputtering and grain-grain collisions. Such destruction can return large amounts of heavy elements such as silicon to the gas. As this is readily converted to SiO, emission from this molecule acts as a good tracer of grain erosion in shock waves.

Consider, for the moment, a plane-parallel, hydrodynamic shock wave propagating at velocity v_s through gas in which the magnetic field, B_0, is neglected. In the frame of reference in which the shock front is stationary, the relationship between the upstream and downstream properties depend only on the distance from the shock front and can be found by solving the Rankine–Hugoniot conditions for the conservation of mass, momentum and energy. For a pressure-density relation of the form $P \propto \rho^{\gamma}$ and a strong shock, defined by the Mach number $M_0 = v_s/c_0 >> 1$, where c_0 is the sound speed, one finds $\rho_1/\rho_0 = (\gamma+1)/(\gamma-1)$, and

$$T_1 = \left[\frac{2(\gamma-1)}{(\gamma+1)^2}\right]\left(\frac{\mu m_H}{k}\right)v_s^2 \qquad (69)$$

where subscript '0' refers to upstream gas and '1' to downstream gas. Thus for an adiabatic shock in atomic or cold molecular hydrogen gas, $\gamma = 5/3$ and the gas density increases by a factor of 4 as the gas traverses the shock front. Its immediate post-shock velocity is $0.75v_s$ and post-shock temperature $T_1 \sim 2500$ K for atomic gas and ~3400 K for H_2 for $v_s = 10$ km s^{-1}. For an isothermal shock, in which the excess energy is radiated away, then the post-shock density is proportional to the Mach number of the shock and can be very large. Such highly compressed gas moves at the shock speed and forms a thin shell, with a typical width of $\sim 10^{12}$–10^{14} cm, of swept-up, high density gas at the shock front.

For a shock propagating into H_2 gas in which rotations but not vibrations are excited, that is, for $T_0 \sim 170$–6000 K, $\gamma = 7/5$, the gas density increases by a factor of 6 and $T_1 \sim 3500$ K for a 10 km s^{-1} shock.

Magnetic fields generally play a role in the propagation of shocks since the interstellar gas is always ionized to some degree by UV photons, x-rays and cosmic ray particles. When the ionization fraction is high and the charged particles are well-coupled to each other, to the neutral gas and to the magnetic field, the 'frozen field' approximation is often adopted. This depends on the ions, electrons and neutral particles being well-coupled through collisions that transfer momentum between the gas particles. While ion-electron collisions in dense interstellar clouds are fast, the low fractional ionization, $\sim 10^{-7}$–10^{-8}, for a cloud with number density, $n \sim 10^4$ cm^{-3}, means that the coupling between ions and neutrals is weak and the compression of the magnetic field by the shock is not transmitted to the neutral gas. The poor coupling between ions and neutrals results in an extended region, much larger than the neutral-neutral collision length, in which ion magnetosonic waves propagate at velocities, v_{ims}, larger than the shock velocity v_s, the so-called 'magnetic precursor', in which the charged and neutral fluids have different temperatures and velocities. In particular, for conditions appropriate to the interstellar medium, the shock does not cause a discontinuity—a jump or J-shock—and physical parameters in the pre- and post-shock gas are connected in a continuous manner, a so-called C-shock. The presence of a C-shock can have important consequences for the chemistry since ion-neutral streaming can overcome activation energy barriers and reaction endothermicities and the interaction region, L, can be much larger than that in hydrodynamic J-shocks. The length scale is given by Flower *et al* (1986) and Draine (1980):

$$L = \frac{(\mu_n + \mu_i)B_0^2}{\pi\rho_{i0}\rho_{n0} < \sigma v > v_s} \qquad (70)$$

where $\mu_{n,i}$ are the neutral and ionized masses respectively. Since $L \propto 1/\rho_{i0}$, L can be quite large for the low-ionized environments of molecular clouds.

Indeed, there is important feedback from the chemistry on the shock structure since fast ion-neutral chemistry can lead to additional neutralisation of the gas. An example is the endothermic reaction:

$$C^+ + H_2 \longrightarrow CH^+ + H + \Delta E \quad (\Delta E/k = 4640\,\mathrm{K}) \quad (71)$$

followed by:

$$CH^+ + e \longrightarrow C + H \quad (72)$$

which leads, in diffuse molecular gas in which C^+ is the most abundant ion, to a reduction in the overall fractional ionization of the gas.

Molecular gas cools very rapidly once the shock front passes, on a time scale of a few tens of years, so any region of hot, very dense, shock-processed gas is relatively thin by astronomical standards. For example, for a non-MHD shock, one can calculate analytically the column density of CH^+, $N(CH^+)$, in the post-shock gas, that is, the number density of CH^+ per unit volume integrated along the line of sight through the shock front, if one assumes that it is formed by reaction (71) above and destroyed by exothermic reaction with H_2 (which is faster than dissociative recombination with electrons in many cases) then one finds:

$$N(CH^+) = n_0 v_s \tau_c f_0(C^+) E_1(\Delta E/kT_{ps}) \quad (73)$$

where n_0 is the pre-shock number density (cm^{-3}), v_s is the shock velocity, τ_c the cooling time, $f_0(C^+)$, the initial, pre-shock fractional abundance of C^+, $E_1(y)$ the exponential integral of the first kind, and T_{ps} the immediate post-shock temperature. Here we have assumed that the post-shock gas cools exponentially from T_{ps} in time τ_c. Since $N_0(C^+)$, the column density of C^+ swept up by the shock front in one cooling time, is given by:

$$N_0(C^+) = n_0 v_s \tau_c f_0(C^+) \quad (74)$$

we see that the value of the exponential integral measures the efficiency by which C^+ is converted to CH^+.

Pineau des Forêts *et al* (1986) have calculated the column density of CH^+ produced in transverse hydrodynamic and MHD shocks impinging on diffuse interstellar clouds, that is, gas at low number density such that UV photons are able to maintain a rather high fractional ionization, $\sim 10^{-4}$–10^{-5}, in the pre-shock gas. For a hydrodynamic shock speed of 10 km s^{-1} and an initial density of 20 hydrogen nuclei cm^{-3}, they calculate an immediate post-shock temperature of 3060 K and a column density, $N(CH^+) = 10^{12}$ cm^{-2} for physical conditions appropriate for clouds in which the column density is observed to be greater than 10^{13} cm^{-2}.

Pineau des Forêts *et al* (1986) also calculated the effect of including a magnetic induction of $B_0 = 5$–12 μG. The neutrals, ions and electrons can thus possess independent velocities and temperatures. For a 10 km s^{-1} shock and $B_0 = 5$ μG, they calculate a maximum neutral gas temperature of 925 K and a maximum ion-neutral drift velocity of 4.6 km s^{-1} over a length scale in which the ions and neutrals are decoupled, $L = 1.4\ 10^{17}$ cm. Despite the much lower temperatures post-shock, the differential motion of the ions and neutrals is sufficient to overcome the endothermicity of the $C^+ - H_2$ reaction. The large length scale over which decoupling occurs leads to a CH^+ column density of 10^{13} cm^{-2}, that is, the inclusion of magnetic fields on the shock structure drives the chemistry more efficiently and leads to column densities much enhanced over the non-MHD models and close to those observed, at least for those species for which endothermic ion-neutral reactions control their chemistry.

In the real world of course, there are many geometries and other parameters, including time-dependence of the underlying source of energy or momentum, to consider but the overall conclusion remains. MHD shocks can induce an ion-neutral drift over an extended region of space and the relative velocity of colliding partners can drive endoergic reactions, overcome activation energy barriers and result in enhanced abundances of molecules that would otherwise be difficult to produce.

3. Astrochemistry in other environments

Although the chemistry discussed to date has concentrated on those regions associated with star formation, molecules also play an important role in other astrophysical regions in which gas-phase, plasma reactions can be important. In this section, we discuss two such regions, the early universe in the first 1000 Myr after the Big Bang and in the circumstellar envelopes of old, dying stars.

3.1. Early universe

The conventional picture of the origin of the Universe starts with the Big Bang out of which space and time, and the elements which form the material Universe, were created. In this expanding and cooling Universe, collisions of protons, neutrons and electrons were fast enough to create only the light elements—H, He, Li and their isotopes most importantly—before the expansion effectively 'froze' nucleosynthesis. Astronomers measure distances in the Universe through the *cosmological redshift*, z, due to the expansion of the Universe, as:

$$1 + z = \frac{\lambda_o}{\lambda_e} \quad (75)$$

where λ_e and λ_o are the wavelengths of the emitted and observed light. The relationship between redshift and the age of the Universe at the point the light was emitted depends on the details of the cosmological model that one adopts but is proportional to $z^{-3/2}$ for large z. As the Universe expanded, the initial plasma cooled and recombined in the so-called 'recombination era', which began at a redshift, z, of about 800–1000, or around five hundred thousand years after the Big Bang, when the gas temperature had fallen to ~8000 K, and continued to its re-ionization due to the first generation of massive stars at $z \sim 15$, at an age of about 250 Myr. In this era, molecular hydrogen formed through gas-phase processes involving H^+:

$$H^+ + H \longrightarrow H_2^+ + h\nu \quad (76)$$

$$H_2^+ + H \longrightarrow H_2 + H^+ \quad (77)$$

and H^-:

$$H + e \longrightarrow H^- + h\nu \quad (78)$$

$$H^- + H \longrightarrow H_2 + e. \quad (79)$$

These two routes tend to occur at different redshifts because the H^- ion is more easily destroyed by photons than H_2^+ and is not abundant until the Universe has cooled sufficiently to prevent the formation of high-energy photons. Formation of H_2 via H^+ peaks at $z \sim 400$ and via H^- at $z \sim 100$. These specific reactions have slow, rate-limiting steps so that the amount of H_2 formed is small, with a fractional abundance of $\sim 10^{-6}$. Other molecules also form, notably HD and LiH, in reactions such as:

$$H^+ + D \longrightarrow H + D^+ \quad (80)$$

$$D^+ + H_2 \longrightarrow HD + H^+ \quad (81)$$

$$Li + H \longrightarrow LiH + h\nu. \quad (82)$$

The abundance of such molecules remains small but because both possess a permanent electric dipole moment they are able to contribute to the cooling of the gas. H_2 is, however, the dominant coolant and the gas cools from ~4000 K to ~200 K. This large decrease in temperature causes a reduction in the internal pressure of the gas and, despite the fact that the Universe itself is expanding, this reduction allows gravitational collapse to proceed and the first stars and galaxies to form. An excellent review of the chemistry in pre-galactic gas and in the mini-haloes of proto-galaxies can be found in Glover (2011). He shows that, since the density and temperature of the Universe is changing with time, the detailed cooling of the gas and the masses of the structures which form are very sensitive to the particular values of the rate coefficients over a wide range of temperature. An extensive review of the chemistry of the light atoms created in the Big Bang is given by Galli and Palla (2013).

The first generation of stars in the Universe is then able to produce the heavier elements—C, N, O, etc—through stellar nucleosynthesis and return these elements to the interstellar medium through supernova explosions and stellar winds. Although we do not detect the first molecules to form, HD and LiH, the molecule CO has been detected in several galaxies out to redshift of 6 (Wang *et al* 2010). The record is in the quasar SDSS J1148 + 5251 at $z = 6.42$, some 890 Myr after the Big Bang (Walter *et al* 2003). This object has over $10^{10} M_\odot$ of molecular gas and is forming stars at a rate of 3000 $M_\odot$ yr^{-1}, roughly 1000 times the value in the Milky Way.

3.2. Circumstellar envelopes

Molecules also form very efficiently in cool stars. Stars with masses in the range 1–8 $M_\odot$ end their lives through losing mass in a stellar wind to the interstellar medium—higher mass stars become supernovae and return material explosively. At the end of their nuclear-burning phase, the stars are very large, with photospheric radii on the order of 200–300 $R_\odot$, and relatively cool with effective temperatures of 2000–3000 K, and are known as asymptotic giant branch (AGB) stars. These winds, which typically have velocities of 10–25 km s^{-1}, eventually, over a few 10 000 yrs, remove the outer layers of the stellar atmosphere to form a planetary nebula with a central, hot, white dwarf star.

The nature of the molecules and the chemistry that occurs in the circumstellar envelopes (CSEs) formed by the mass loss depends on the overall carbon-to-oxygen, C/O, ratio and on the properties of three main radial zones around the central star. These CSEs can be very rich in molecules, particularly those which are carbon-rich: the archetype of these, the star IRC+10216 or CW Leo, with a mass loss rate of 2 10^{-5} $M_\odot$ yr^{-1} and an expansion velocity of 14.5 km s^{-1}, contains over 80 molecules including many carbon-chain species, as found in dark clouds, and several metal halides including NaCl, KCl and AlCl, molecules yet to be detected in interstellar clouds.

The chemistry occurring in CSEs can be considered to proceed in three regions delineated by radial distance from the central star, which has a photospheric (stellar) radius, R_*, of a few 10^{13} cm. It should be noted that stellar UV photons are unimportant in the chemistry since the stars are cool.

3.2.1. Photospheric chemistry. At the high densities, more than 10^{13} cm^{-3}, and temperatures experienced at the photosphere, typically 2500–3500 K, too hot for dust grains to survive, molecules are formed in *local thermodynamic equilibrium* (LTE). Three-body collisions among neutral species dominate—one of the few astrochemical situations where this is the case—and molecular abundances are determined by minimising the Gibbs free energy:

$$G = \Sigma f_i x_i \quad (83)$$

where x_i is the number of moles of species i and f_i its chemical potential:

$$f_i = \left(\frac{G}{RT}\right)_i + \ln P + \ln\left(\frac{x_i}{\bar{x}}\right) \quad (84)$$

with $(G/RT)_i$ the Gibbs free energy of species i, P the total pressure of the gas, and $\bar{x} = \Sigma x_i$. LTE preferentially forms molecules with high dissociation energies, in particular CO is the most abundant molecule after H_2 for conditions typical of C-rich and O-rich AGB stars. In C-rich stars, essentially all available oxygen is tied up in CO (bond energy 11.2 eV). The excess carbon ends up in abundant species such as C_2H_2, HCN and CS, with nitrogen partitioned into molecules such as N_2 and HCN. Observations of all these species, with the exception of N_2, can be made close to the photosphere through infrared absorption and emission spectroscopy. In O-rich stars, CO, H_2 O and SiO are the most abundant O-bearing species.

In modelling the chemistry of AGB stars, it is often the case that LTE calculations are used to set the abundances of 'parent' species which then flow out into the outer regions of the CSE. There are, however, two major processes which perturb the LTE abundances.

3.2.2. Pulsations and dust formation. The inner regions of the CSE are not stable structures since AGB stars pulsate on time-scales of 1–3 years, typically. These sub-sonic pulsations generated in the interior of the star drive compression waves through the atmosphere steepening into shocks. Such shocks lose energy either radiatively, when the density is high and the shocks can be treated as isothermal, or by adiabatic expansion when the density is low. Detailed models of these shocks have been made by Bowen (1988) who showed that strong shocks occur on a cyclic basis and create an extended atmosphere in which the shock velocity decreases as the gas expands. A particular parcel of gas which receives an outward impulse roughly follows a ballistic trajectory before falling back towards the stellar surface under the influence of gravity. If it experiences a second shock before it returns to its initial position, it attains a net outward momentum and can drive mass loss.

Willacy and Cherchneff (1998) studied the chemistry in the inner 5 R_* induced by these periodic shock waves on a molecular gas whose initial composition is determined by LTE. The chemistry is dominated by neutral–neutral reactions which, if they can occur faster than the dynamical time-scales, can alter LTE abundances dramatically. Key reactants at these high temperatures and densities are atomic hydrogen and O atoms formed by collisional dissociation of H_2 and CO. In C-rich stars, these O atoms can react with H_2 to form OH and H_2O, while atomic silicon, the dominant form of the element in LTE, reacts with OH to form SiO, increasing the latter abundance by more than a factor of 100 compared to its LTE value and giving closer agreement with the abundance observed close to the photosphere.

Shock chemistry, driven by underlying pulsations, does seem to be required to explain the relatively high abundances of O-bearing molecules, including OH, H_2O and H_2CO, detected in IRC+10216 in recent years. Cherchneff (2012) gives an excellent summary of the physics and chemistry of this inner region and shows that, in addition to O-bearing molecules, shock chemistry can produce large abundances of chlorides such as HCl, AlCl and NaCl, as also observed.

AGB stars are also the major producer, perhaps up to 80%, of dust particles in the Galaxy. Infrared observations show that the dust composition is either amorphous carbon in C-rich stars or silicates in O-rich stars. The formation of these are not well understood although it is clear that it occurs within a few stellar radii. Initial research on dust formation in carbon stars invoked classical nucleation theory in which solids condense out of a cooling gas once the partial pressure of a particular species exceeds its vapour pressure. Nucleation theory describes growth from gas-phase monomers and identifies a critical cluster size above which growth by addition of a monomer is energetically favoured. This approach has had only limited success in its application to AGB stars. For O-rich stars, there is no monomer out of which the observed silicates can grow whilst in C-rich stars, there are kinetic bottlenecks in the formation of the first few ring molecules, and in both types the short dynamical time-scales can mitigate against grain formation. Pulsations again seem to be critical. The levitation of material in the atmosphere, the density increase caused by the propagation of shock waves, and the fast cooling post-shock, have been included in a kinetic description of the chemistry in C-rich stars (Cherchneff (2012) and references therein). In this model for IRC+10216, she showed that the abundance of benzene peaked at a fractional abundance of 10^{-6} at around 3 R_*. Assuming that benzene is converted to coronene, $C_{24}H_{12}$, through a series of H-abstraction, acetylene-addition reactions, and that this is a proxy for the dust mass, she showed that dust masses consistent with those observed can be achieved.

In O-rich stars, the dominant dust component is amorphous silicate with evidence also for crystalline silicates. The most abundant oxide in the gas after CO in the dust-forming zone is SiO which has a condensation temperature of around 600 K, much lower than the observed dust temperature, around 1000 K. It is thus likely to be the more refractory oxides, such as TiO, TiO_2, AlO and Al_2O_3, which form the first condensates on which further grain growth can occur. Corundum, Al_2O_3, is the most abundant Al-containing molecule and can condense out of the gas below 1000 K (Sharp and Huebner 1990)—some 90% of all pre-solar oxide grains found in meteorites contain corundum that condensed in O-rich AGB stars. LTE conditions, however, are unlikely to hold given stellar pulsations and the generation of periodic shock waves but the identification of the detailed chemical reactions that form the smallest molecular clusters is still elusive. Kinetic models of the chemistry are difficult to describe although Gail and Sedlmayr (1998) have shown that solid TiO_2 may provide the seed nuclei on which silicates condense—the low abundance of Ti compared to Si and Mg, however, may be problematic in this scenario. Goumans and Bromley (2012) have investigated the thermodynamics of small cluster formation in a 1000 K gas of H_2, SiO, Mg and H_2O and find that the homomolecular nucleation of SiO stops at the dimer, whereas Mg can be incorporated exothermically into silicon oxides when the number of oxygen atoms is larger than that of the metal atoms.

Once formed, dust grains become the most important absorber of stellar photons and the transfer of photon momentum to the dust, and subsequently to the gas through collisions, initiates a rapid acceleration of the gas and drives the mass-loss process. As the gas and dust flows outwards, collisions between them are possible although a comparison between the gas-grain collision time and the expansion time shows that this is important only within 10^{15} cm for typical conditions. There has been, as yet, little attempt to study the gas-dust interaction in this zone, where both the gas and the grains are hot, but there is evidence that molecule formation mediated by this interaction does occur. For example, 10 μm observations of silane, SiH_4, in IRC+10216 (Keady and Ridgway 1993) shows that it is formed at radii beyond 40 R_*—similar results hold for CH_4 and NH_3. The increased abundances of these and other hydrides in this region may imply, as it does in the case of hot molecular cores, that molecules are being formed on the surfaces of dust grains through hydrogenation of atoms, although other explanations are possible.

Consider H_2O which was detected in IRC+10216 through submillimetre satellite observations (Melnick *et al* 2001). This observation was a surprise since neither the LTE models for the inner chemistry nor the models of the outer CSE

predicted water. This observation, which was followed by observations of OH and H_2CO in the same star, led to suggestions that water was formed by the evaporation of icy comets orbiting within the CSE (Melnick *et al* 2001), or that it could be formed in the dust growth zone by the Fischer–Tropsch mechanism on the surface of iron grains (Willacy 2004). Subsequent observations of high-excitation transitions using the Herschel Space Observatory (Decin *et al* 2010) showed unequivocally that water is warm, several hundred K, and confined to the inner envelope. Cherchneff (2011) argued that this is consistent with recent shock models, although several of the key rate coefficients are unknown or highly uncertain. Agúndez *et al* (2010) used the observed clumpy nature of the CSE to postulate that external UV photons can penetrate deep into the inner regions of the envelope and drive the photodissociation of molecules such as SiO and ^{13}CO which release O atoms into the gas phase—^{12}CO is optically thick to dissociating photons. The O atoms then react with H_2 in the warm gas to form OH and water.

3.2.3. Photochemistry in the outer envelope. In the very outer reaches of the circumstellar envelope, external UV photons can disrupt the chemistry, giving rise a rich soup of radicals and ions that can react further. An interesting outcome in some CSEs, as discussed below, is that the chemistry produces relatively high abundances of anions, one of the few regions in the ISM in which they are formed in observable quantities.

To understand the underlying physical properties and chemistry of the gas, let us assume that gas and dust flow out from the star in a steady, uniform, spherically symmetric flow at terminal velocity v and mass-loss rate $\dot{M}$ and which is irradiated by external UV photons from the interstellar radiation field. In this case, we can use conservation of mass to derive the H_2 abundance as a function of radius. We can then write the radial number density of H_2, $n(H_2, r)$, the radial column density of H_2 from radial distance r to infinity, $N(H_2, r)$, and the radial extinction in the UV due to dust, $A_{UV}(r)$ as:

$$n(H_2, r) = 7.1 \times 10^4 \left(\frac{\dot{M}}{10^{-5}}\right)\left(\frac{10^{16}}{r}\right)^2\left(\frac{15}{v}\right) \text{cm}^{-3} \quad (85)$$

$$N(H_2, r) = 7.1 \times 10^{20} \left(\frac{\dot{M}}{10^{-5}}\right)\left(\frac{10^{16}}{r}\right)\left(\frac{15}{v}\right) \text{cm}^{-3} \quad (86)$$

$$A_{UV}(r) = 7.6 \left(\frac{\psi}{0.01}\right)\left(\frac{\dot{M}}{10^{-5}}\right)\left(\frac{10^{16}}{r}\right)\left(\frac{15}{v}\right) \text{mag}. \quad (87)$$

Here the mass-loss rate is measured in $M_\odot$ yr^{-1}, the radial distance in cm, the terminal velocity in km s^{-1} and ψ is the dust-to-gas mass ratio, where 0.01 is its typical value in the interstellar medium. It is likely to vary from object to object in AGB stars, with a typical value of perhaps 0.003. The temperature profile of the gas is determined by adiabatic expansion and molecular line and dust thermal cooling but can be well approximated by a power-law distribution $T(r) \propto r^{-\alpha}$, with α around 0.6–0.7. At an injection radius of 2 10^{15} cm, the H_2 density is about 3 10^6 cm^{-3}, the temperature is 220 K and the radial visual extinction, A_V, about 7 mag, for parameters typical of those in IRC+10216 (McElroy *et al* 2013).

One sees from these equations, that since external UV photons begin to interact with outflowing parent species once the UV extinction falls below about 10 mags, that is, at a radius of around 10^{16} cm for parameters typical of AGB stars. One should note, however, that three of the major parent species, namely H_2, N_2 and CO experience self- and mutual-shielding against photodestruction. Indeed the H_2 photodissociation rate is negligible to distances typically in excess of 1 parsec (3.086×10^{18} cm) from the star. In C-rich AGB stars, the most important parents for driving chemistry are C_2H_2 and HCN. The photodissociation of HCN gives rise to CN which is itself photodissociated to N and C atoms, with the latter photoionized in the very outer envelope. Thus, external photons cause the formation of molecular shells, whose radial position depend on the underlying flow properties and the photon flux. Acetylene can be both ionized, to form $C_2H_2^+$, and dissociated, to form C_2H, C_2, C and C^+, sequentially. The result is that one finds a region in the CSE where abundant photons, radicals and ions co-exist at relatively high density, $n(H_2) \sim 10^4$ cm^{-3}, and cold temperatures, 100–10 K, a situation that is relatively rare in astronomy. Collisions between these reactive species then give rise to the molecular complexity observed in C-rich CSEs through reactions described in section 2.2.

One of the interesting aspects of the chemistry is its propensity to form carbon-chain molecules and anions—CN^-, C_3N^-, C_5N^-, C_4H^-, C_6H^-, C_8H^- have been detected in IRC+10216—in relatively high abundance; indeed the total anion abundance is found to exceed that of free electrons in some parts of the outer envelope (Millar *et al* 2007, Cordiner and Millar 2009). Figure 16 from McElroy *et al* (2013) shows the radial distributions of a number of important linear hydrocarbon molecules and anions. We note that in IRC+10216, the observed ratios for C_6H^-/C_6H and C_8H^-/C_8H are 0.09 and 0.26, respectively (Kasai *et al* 2007, Remijan *et al* 2007).

The cyanopolyynes, $HC_{2n+1}N$ are formed via neutral-neutral reactions between CN and the polyynes:

$$C_{2n}H_2 + CN \longrightarrow HC_{2n+1}N + H. \quad (88)$$

Large carbon-chain molecules often possess large electron affinities and can undergo radiative attachment with electrons, with rate coefficients that generally increase with size of the neutral (Herbst and Osamura 2008). Thus C_6H^-, because of the relatively large abundance of C_6H and fast radiative attachment of electrons to C_6H, is the dominant anion in the outer CSE. The formation of the cyanopolyyne anions occurs by radiative attachment as well as through reactions between N atoms and anions (Eichelberger *et al* 2007):

$$C_nH^- + N \longrightarrow C_nN^- + H \quad (89)$$

$$C_n^- + N \longrightarrow CN^- + C_{n-1}. \quad (90)$$

Figure 16, top right panel, shows the interesting result that the presence of these large hydrocarbon anions act to enhance the formation of large hydrocarbon chain molecules in the outer CSE as noted previously for dark clouds (Walsh *et al* 2009). A unique impact on the CSE chemistry, however, is

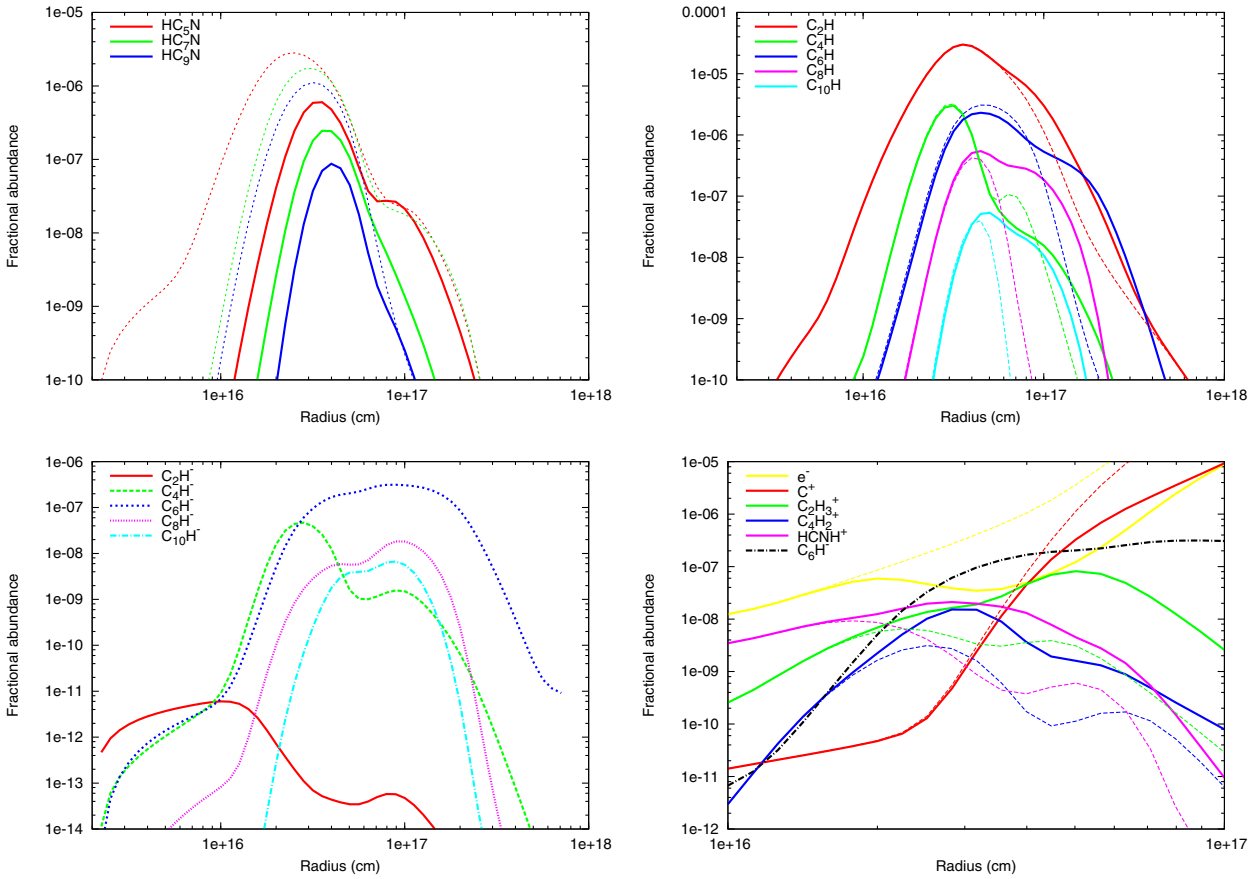

Figure 16. Top left: plot of the fractional abundances, relative to H_2, of cyanopolyynes as a function of envelope radius using the Rate12 model (solid lines) compared with the results from Cordiner and Millar (2009) (dotted lines). Top right: Plot of fractional abundances of polyynes as a function of envelope radius for the Rate12 model including anion chemistry (solid lines) and excluding anion chemistry (dashed lines). Bottom left: plot of fractional abundances of polyyne anions as a function of envelope radius. Bottom right: comparison of the fractional abundances of various cations and electrons, including anion chemistry (solid lines) and excluding anion chemistry (dashed lines). The C_6H^- fractional abundance for the 'anions included' model is shown, for reference, with a dot-dashed line (McElroy *et al* (2013) © ESO.)

that the free electron abundance can be depressed by an order of magnitude below the anion abundance in the range 0.3–1.0 10^{17} cm in figure 16. This reduction in electron abundance leads to the decreased importance of dissociative electron recombination as a loss mechanism for cations, see the lower right panel in figure 16, with cations increasing in abundance by factors of 10–1000. The lower right panel also shows the radial abundance of C_6H^- which is the dominant carrier of negative charge in the region 3–6 10^{16} cm.

The chemical reactions that synthesise molecules in the CSE are thus identical to those occurring in cold dark clouds. In the latter, however, the chemistry is acting to transform atoms to molecules, whereas in the envelopes of AGB stars, the chemistry acts to transform stable molecules formed in and near the photosphere to atoms and atomic ions which return to the interstellar medium to begin the process of cloud formation and collapse, star and planet formation, stellar evolution and star death, and another cycle in the history of chemistry in the Galaxy.

4. Summary

We have seen that chemistry controls many aspects of the evolution of the Universe, in particular the formation of stars, and that observations of molecular line transitions are powerful probes of physics, in the determination of number densities, temperatures and gas dynamics. Much of the chemistry occurs at temperatures and pressures much less than those experienced in terrestrial laboratories and over time scales of up to one million years. Nevertheless, laboratory experiments are urgently needed to understand important processes and provide key reaction rate coefficients. Among these are dissociative recombination of protonated molecules, particularly large organic molecules, with electrons. Here, the branching ratios are often more important to know than the overall rate coefficient. As an example, protonated methanol produces methanol in only 3% of its dissociative recombinations with electrons (Geppert *et al* 2006) rather than the 50% normally assumed in models at that time. This low branching ratio is not sufficient to produce methanol at its observed abundances in molecular clouds (Wirström *et al* 2011). It indicates, rather, that methanol is produced through the hydrogenation of CO in icy grain mantles, consistent with the detection of CD_3OH (Parise *et al* 2004) and laboratory experiments on the surface chemistry of CO with D and H atoms (Watanabe *et al* 2004, Hidaka *et al* 2009). Other protonated species which have very small branching ratios to their parent neutral include protonated ethanol and protonated dimethyl ether (Hamberg *et al* (2010a),

2010b) but not all dissociative recombinations of protonated COMs are inefficient, propionitrile is produced in 43% of recombinations (Vigren *et al* 2010). Laboratory studies of the rate coefficients and branching ratios of the dissociative recombination of protonated COMs and other large molecular ions, for example PAH cations, remain an important topic in astrochemistry.

The recent detection of anions and the conclusion that they could be more abundant than free electrons in some regions (section 3.2.3), implies that it will also be important to study cation–anion recombinations. A number of processes involving anions still remain relatively unexplored at low energies in the laboratory. These include processes such as radiative attachment, associative electron detachment and mutual neutralisation. In cold dark molecular clouds, it is likely that the population of PAH-like molecules (section 1.2) are negatively charged; here again, laboratory studies of their reactions with atoms, radicals, neutral molecules and cations are lacking, although Bierbaum and colleagues have made some important measurements on the reactivities of PAH cations and anions (Demarais *et al* 2012, 2014). Such reactions may also have particular relevance to astrobiology.

The interaction of UV photons and cosmic ray particles with the gas means that chemical reactions are predominantly ion-neutral in nature, such processes contributing to the enormous isotope enhancements that are detected in deuterated species. The chemistry of the interstellar medium is, however, not restricted to the gas phase and reactions in and on the icy mantles of grains, although very poorly understood at present, do seem to be critical in the formation of complex organic molecules in star-forming regions. Significant work needs to be done to better understand the mechanisms by which photons and high-energy electrons and cosmic-ray protons interact with water ice and the mixed and layered ices thought to be present in the ISM. There remains uncertainty over the competition between dissociation of ice molecules, which can create reactive radicals and ions in the ice, the reactive pathways that ions, in particular, may follow and the desorption of these radicals and their parents. Binding energies and diffusion barriers control the mobility and reactivity of material in the ice and are a particular source of uncertainty given the exponential dependence of relevant time scales on these parameters. Many models of grain surface chemistry assume the same energetics and outcomes as gas-phase chemistry—the dissociative recombination of molecular ions on the surfaces of negatively charged grains is one such example—and must surely be a source of great uncertainty in modelled outcomes. Finally, we note that the characteristics of the grains themselves must play a key role in the chemistry through their composition, porosity, size distribution, for example. It is clear from current experiments that the ice chemistry is complex although still ill-defined in a global sense. We may have some ideas and a reasonable degree of certainty as to how simple species such as water and methanol form through hydrogenation of O and CO respectively, but we have much less confidence in describing how complex molecules form on grains. Current chemical kinetic models contain several thousand gas-phase reactions and only a few hundred surface reactions. It is likely that chemistry in the bulk ice needs to be considered more fully given that energetic interactions happen here rather than in the surface layer and that many hundred, if not thousands, of ice reactions need to be included—a very challenging task.

The challenge, however, may have great rewards. Evidence from the laboratory, from the composition of meteorites and from the *Stardust* comet return mission indicate that complex molecules, including many amino acids and nucleobases, can be readily formed under conditions similar to those present in interstellar clouds. Can these pre-biotic molecules help the emergence of life in our own and other solar systems? A continuing close collaboration between astronomers, chemists and physicists—and biologists—may provide the answer to this within the lifetime of our current graduate students.

Acknowledgments

Molecular Astrophysics at QUB is supported by a grant from the Science and Technology Facilities Council. I am very grateful to the referees whose careful reading and comments improved this article.

References

Agúndez M, Cernicharo J and Guélin M 2010 *Astrophys. J.* **724** L133
Barlow M J *et al* 2013 *Science* **342** 1343
Barzel B and Biham O 2012b *Phys. Rev.* E **86** 031126
Barzel B and Biham O 2011 *Phys. Rev. Lett.* **106** 150602
Barzel B, Biham O, Kupferman R, Lipshtat A and Zait A 2010 *Phys. Rev.* E **82** 021117
Bowen G H 1988 *Astrophys. J.* **329** 299
Brown P D and Millar T J 1989 *Mon. Not. R. Astron. Soc.* **237** 661
Cami J, Bernard-Salas J and Peeters E 2010 *Science* **329** 1180
Caselli P, Hasegawa T I and Herbst E 1998 *Astrophys. J.* **495** 309
Cazaux S and Tielens A G G M 2002 *Astrophys. J.* **575** L29
Charnley S B 1998 *Astrophys. J.* **509** L121
Chen Y-J, Ciaravella A, Muñoz Caro G, Cecchi-Pestellini C, Jiménez-Escobar A, Juang K-J and Yih T-S 2013 *Astrophys. J.* **778** 162
Cherchneff I 2011 *Astron. Astrophys.* **526** L11
Cherchneff I 2012 *Astron. Astrophys.* **545** A12
Ciaravella A, Jiménez-Escobar A, Muñoz Caro G, Cecchi-Pestellini C, Candia R, Giarrusso S, Barbera M and Collura A 2012 *Astrophys. J.* **746** L1
Cordiner M A and Millar T J 2009 *Astrophys. J.* **697** 68
Croswell K and Dalgarno A 1985 *Astrophys. J.* **289** 618
Crutcher R M 2012 *Ann. Rev. Astron. Astrophys.* **50** 29
Crutcher R M, Hakobian N and Troland T H 2009 *Astrophys. J.* **692** 844
Cuppen H M and Garrod R T 2011 *Astron. Astrophys.* **529** A151
Cuppen H M and Herbst E 2005 *Mon. Not. R. Astron. Soc.* **361** 565
Cuppen H M and Herbst E 2007 *Astrophys. J.* **668** 294
Cuppen H M, Karssemeijer L J and Lamberts T 2013 *Chem. Rev.* **113** 8840
Decin L *et al* 2010 *Nature* **467** 64
Demarais N J, Yang Z, Martinez O, Wehres N, Snow T P and Bierbaum V M 2012 *Astrophys. J.* **746** 32
Demarais N J, Yang Z, Snow T P and Bierbaum V M 2014 *Astrophys. J.* **784** 25
Draine B T 1980 *Astrophys. J.* **241** 1021

Drozdovskaya M N, Walsh C, Visser R, Harsono D and van Dishoeck E F 2014 *Mon. Not. R. Astron. Soc.* **445** 913
Eichelberger B, Snow T V, Barckholtz C and Bierbaum V M 2007 *Astrophys. J.* **667** 1283
Elsila J E, Glavin D P and Dworkin J P 2009 *Meteorit. Planet. Sci.* **44** 1323
Favre C, Cleeves L I, Bergin E A, Qi C and Blake G A 2013 *Astrophys. J.* **776** L38
Flower D R, Pineau des Forêts, G and Walmsley C M 2004 *Astron. Astrophys.* **427** 887
Flower D R, Pineau des Forêts G and Hartquist T W 1986 *Mon. Not. R. Astr. Soc.* **218** 729
Fogel J K, Bethell T J, Bergin E A, Calvet N and Semenov D 2011 *Astrophys. J.* **726** 29
Furuya K, Aikawa Y, Nomura H, Hersant F and Wakelam V 2013 *Astrophys. J.* **779** 11
Gail H-P and Sedlmayr E 1998 *Farad. Disc.* **109** 303
Galli D and Palla F 2013 *Ann. Rev. Astron. Astrophys.* **51** 163
Garrod R T and Herbst E 2006 *Astron. Astrophys.* **457** 927
Geppert W D *et al* 2006 *Faraday Trans.* **133** 177
Gibb E L *et al* 2000 *Astrophys. J.* **536** 347
Gillespie D T, Hellander A and Petzold L R 2013 *J. Chem. Phys.* **138** 170901
Glover S C O 2011 *The Molecular Universe* Cernicharo J, Bachiller R (Cambridge: Cambridge University Press) p 313
Goumans T P M and Bromley S T 2012 *Mon. Not. R. Astron. Soc.* **420** 3344
Hamberg M *et al* 2010a *Astron. Astrophys.* **522** A90
Hamberg Österdahl F *et al* 2010b *Astron. Astrophys.* **514** A83
Heinzeller D, Nomura H, Walsh C and Millar T J 2011 *Astrophys. J.* **731** 115
Henning Th and Semenov D 2013 *Chem. Rev.* **113** 9016
Herbst E and Osamura Y 2008 *Astrophys. J.* **679** 1670
Herbst E and van Dishoeck E F 2009 *Ann. Rev. Astron. Astrophys.* **47** 427
Hidaka H, Watanabe M, Kouchi A and Watanabe N 2009 *Astrophys. J.* **702** 291
Hincelin U, Wakelam V, Commerçon B, Hersant F and Wakelam F 2013 *Astrophys. J.* **779** 11
Hollenbach D and Salpeter E E 1971 *Astrophys. J.* **163** 155
Hugo E, Asvany O and Schlemmer S 2009 *J. Chem. Phys.* **130** 164302
Indriolo N and McCall B J 2012 *Astrophys. J.* **745** 91
Jørgensen J K, Favre C, Bisschop S E, Bourke T L, van Dishoeck E F and Schmalzl M 2012 *Astrophys. J.* **757** L4
Ilee J, Boley A C, Caselli P, Durisen R H, Hartquist T W and Rawlings J M C 2011 *Mon. Not. R. Astron. Soc.* **417** 2950
Kasai Y, Kagi E and Kawaguchi K 2007 *Astrophys. J.* **661** L61
Keady J J and Ridgway S T 1993 *Astrophys. J.* **406** 199
Laas J C, Garrod R T, Herbst E and Widicus Weaver S L 2011 *Astrophys. J.* **728** 71
Lee J-E, Bergin E A and Nomura H 2010 *Astrophys. J.* **710** L21
Lee T, Papanastassiou D A and Wasserburg G J 1977 *Astrophys. J.* **211** L107
Lipshtat A and Biham O 2004 *Phys. Rev. Lett.* **93** 170601
Lis D C, Roueff E, Gerin M, Phillips T G, Coudert L H, van der Tak F F S, van der Tak F F S and Schilke P 2002 *Astrophys. J.* **571** L55
Lynden-Bell D and Pringle J E 1974 *Mon. Not. R. Astron. Soc.* **168** 603
McElroy D, Walsh C, Markwick A J, Cordiner M A, Smith K and Millar T J 2013 *Astron. Astrophys.* **550** A36
Melnick G J *et al* 2001 *Nature* **412** 160
Millar T J, Walsh C, Cordiner M A, Ní Chuimín R and Herbst E 2007 *Astrophys. J.* **662** L87
Mitchell J B A 1990 *Phys. Rep.* **186** 215
Nomura H and Millar T J 2005 *Astron. Astrophys.* **438** 923
Nomura H, Aikawa Y, Tsujimoto M, Nakagawa Y and Millar T J 2007 *Astrophys. J.* **661** 334
Öberg K I, Boogert A C A, Pontoppidan K M, van den Broek S, van Dishoeck E F, Bottinelli S, Blake G A and Evans II N J 2011 *Astron. Astrophys.* **740** 109
Öberg K I, Garrod R T, van Dishoeck E F and Linnartz H 2009 *Astron. Astrophys.* **508** 891
Oka T 2004 *J. Mol. Spectrosc.* **228** 635
Pagani L, Vastel C, Hugo E, Kokoouline V, Greene C H, Bacmann A, Bayet E, Ceccarelli C, Peng R and Schlemmer S 2009 *Astron. Astrophys.* **494** 623
Parise B, Castets A, Herbst E, Caux E, Ceccarelli C and Tielens A G G M 2004 *Astron. Astrophys.* **416** 159
Parise B, Ceccarelli C, Tielens A G G M, Castets A, Caux E, Lefloch B and Maret S 2006 *Astron. Astrophys.* **453** 949
Parise B, Du F, Liu F-C, Belloche A, Wiesemeyer H, Güsten R, Menten K M, Hübers H-W and Klein B 2012 *Astron. Astrophys.* **542** L5
Pineau des Forêts G, Flower D R, Hartquist T W and Dalgarno A 1986 *Mon. Not. R. Astron. Soc.* **220** 801
Pringle J E 1981 *Ann. Rev. Astron. Astrophys.* **19** 137
Ratchford B L *et al* 2009 *Astron. Astrophys. Suppl. Ser.* **180** 125
Remijan A J, Hollis J M, Lovas F J, Cordiner M A, Millar T J, Markwick-Kemper A J and Jewell P R 2007 *Astrophys. J.* **664** L47
Roberts H, Herbst E and Millar T J 2003 *Astrophys. J.* **591** L41
Roberts H and Millar T J 2006 *Phil. Trans. R. Soc.* A **364** 3063
Roberts H and Millar T J 2007 *Astron. Astrophys.* **471** 849
Schilke P *et al* 2014 *Astron. Astrophys.* **566** A29
Sharp C M and Huebner W F 1990 *Astron. Astrophys. Suppl. Ser.* **72** 417
Sipilä O, Caselli P and Harju J 2013 *Astron. Astrophys.* **554** A92
Sipilä O, Hugo E, Harju J, Asvany O, Juvela M and Schlemmer S 2010 *Astron. Astrophys.* **509** A98
Stantcheva T and Herbst E 2004 *Astron. Astrophys.* **423** 241
Vasyunin A I and Herbst E 2013 *Astrophys. J.* **762** 86
Vigren E *et al* 2010 *Astrophys. J.* **722** 847
Visser R, Doty S and van Dishoeck E F 2011 *Astron. Astrophys.* **534** A132
Walsh C, Harada N, Herbst E and Millar T J 2009 *Astrophys. J.* **700** 752
Walsh C, Nomura H, Millar T J and Aikawa Y 2012 *Astrophys. J.* **747** 114
Walsh C, Millar T J, Nomura H, Herbst E, Widicus Weaver S, Aikawa Y, Laas J C and Vasyunin A I 2014 *Astron. Astrophys.* **563** A33
Walter F, Bertoldi F, Carilli C, Cox P, Lo K Y, Neri R, Fan X, Omont A, Strauss M A and Menten K M 2003 *Nature* **424** 406
Wang R *et al* 2010 *Astrophys. J.* **714** 699
Watanabe N, Nagaoka A, Shiraki T and Kouchi A 2004 *Astrophys. J.* **616** 638
Willacy K 2004 *Astrophys. J.* **600** L87
Willacy K and Cherchneff I 1998 *Astron. Astrophys.* **330** 676
Wirström E, Geppert W D, Hjalmarson Å, Persson C M, Black J H, Bergman P, Millar T J, Hamberg M and Vigren E 2011 *Astron. Astrophys.* **533** A24
Woods P M and Willacy K 2009 *Astrophys. J.* **693** 1360
Woods P M, Slater B, Raza Z, Viti S, Brown W A and Burke D J 2013 *Astrophys. J.* 777 90